

EFFECTS OF MTN ENZYME DEFICIENCY ON *E. COLI* O157:H7 GROWTH AND
VIRULENCE

by

Reece Knippel

A thesis

submitted in partial fulfillment
of the requirements for the degree of
Master of Science in Chemistry
Boise State University

May 2013

© 2013

Reece Knippel

ALL RIGHTS RESERVED

BOISE STATE UNIVERSITY GRADUATE COLLEGE

DEFENSE COMMITTEE AND FINAL READING APPROVALS

of the thesis submitted by

Reece Knippel

Thesis Title: Effects of MTN Enzyme Deficiency on *E. coli* O157:H7 Growth and Virulence

Date of Final Oral Examination: 15 March 2013

The following individuals read and discussed the thesis submitted by student Reece Knippel, and they evaluated his presentation and response to questions during the final oral examination. They found that the student passed the final oral examination.

Ken Cornell, Ph.D. Chair, Supervisory Committee

Kristen Mitchell, Ph.D. Member, Supervisory Committee

Rajesh Nagarajan, Ph.D. Member, Supervisory Committee

The final reading approval of the thesis was granted by Ken Cornell, Ph.D., Chair of the Supervisory Committee. The thesis was approved for the Graduate College by John R. Pelton, Ph.D., Dean of the Graduate College

DEDICATION

I dedicated this thesis to those who never gave up on me. It has been a chaotic and insane ride these last couple years. I am thankful for all the love and support given to me by family, friends, and classmates. Let the completion of this thesis mark the end of one chapter of my life, as well as the beginning of an exciting new one.

ACKNOWLEDGEMENTS

The first acknowledgement is to Dr. Ken Cornell who allowed me to work in his lab for over four years and was the best mentor I could have wanted. I would like to acknowledge Dr. Haiqing Sheng at the University of Idaho for providing the MTN KO strain in *E. coli* O157:H7 as this work would not have been possible without this strain. I would also like to thank the members of my graduate committee, Dr. Kristen Mitchell and Dr. Rajesh Nagarajan for providing feedback and support for this work. Other thanks are due to the late Dr. Robert Kadner at the University of Virginia for supplying the RK4353 strains, and Dr. Brett Finlay at the University of British Columbia for supplying the α -EspB and α -Tir antibodies. I also thank Ms. Raquel Brown for her technical assistance with the confocal microscopy. Finally, I would like to thank all of the undergraduates who assisted on this thesis, especially Allison Eberly for optimizing biofilm production and Meagan Boll for the analysis and sorting of the proteomic data.

I would also like to acknowledge all of the funding sources that supported this research, especially Idaho INBRE (P20RR016454). Other sources of funding include grants from MSTMRI, Merck/AAAS, NSF REU (CHE-1005159), NSF MRI (CHE-0923535), and Dept. of Defense (MRMCW81XWH-09-0588).

ABSTRACT

The bacterial enzyme Methylthioadenosine/S-adenosylhomocysteine (MTA/SAH) nucleosidase (MTN) is involved in methionine and adenine salvage from the by-products of S-adenosylmethionine (SAM, AdoMet) dependent reactions. MTN plays a critical role in alleviating product inhibition of SAM dependent reactions, including methylation reactions and the synthesis of polyamines, vitamins, and autoinducer signals. Due to its absence from humans and its importance to bacterial metabolism, MTN is a potential target for the development of novel antibiotics to treat microbial infections. In this study, a MTN gene knock-out (MTN KO) strain of the pathogen *E. coli* O157:H7 was created to study the impact of MTN activity on bacterial growth, virulence, and autoinducer-dependent events; and to model the effects that would be expected from complete pharmacologic interruption of enzyme activity. *E. coli* O157:H7 was chosen as the topic of study since it is a serious gram-negative pathogen responsible for severe diarrhea that can progress to cause hemolytic uremic syndrome (HUS), and factors influencing its virulence are well known.

The MTN KO strain showed delayed growth, minimal biofilm production, and decreased *in vitro* virulence when compared to the parental wild type (WT) strain. Notably, the MTN KO strain showed a reduced ability to adhere to cultured mammalian cells. An analysis of virulence factor expression showed that the MTN KO strain secreted less Shiga-toxin, type-III secretory proteins, and hemolysin activity than the parental WT strain. Culture supplementation with autoinducer-2 precursor, 4,5-dihydroxy-2,3-

pentanedione (DPD) did not restore the growth or virulence of the MTN KO strain, suggesting that the virulence defect was not the result of a loss of autoinducer-2 signaling. However, culture supplementation with lipoate, thiamine and biotin partially reconstituted the growth and virulence phenotypes of the KO strain to WT levels, indicating that altered vitamin-dependent metabolic activity played a role in the defect. The lipoate- and thiamine-dependent enzymes in the pyruvate dehydrogenase complex were overexpressed in the MTN KO strain, but the enzyme complex showed lower specific activity than the WT strain, suggesting that the ability to synthesize these vitamins was compromised in the KO strain. Other metabolic enzymes (lactate dehydrogenase, alcohol dehydrogenase, glutamate dehydrogenase) were found to have specific activities equal to the WT strain, thus providing release points for excess metabolites in the KO strain.

This study provides support for MTN as a target for antibiotic treatment. Our results indicate that one mechanism by which MTN specific inhibitors could exert their antibiotic effect is by interrupting vitamin dependent processes, particularly in central carbon metabolism. While loss of MTN activity was not bactericidal in this case, the significant reduction in bacterial growth, biofilm formation and virulence suggests that the bacteria treated with MTN inhibitors could have increased susceptibility to traditional antibiotics and the host immune system responses. This supports the incorporation of MTN inhibitors into combination drug therapies with standard antibiotics. Finally, the creation and analysis of a MTN KO strain provides a valuable tool to explore potential mechanisms of antibiotic action that can be used in comparative studies to examine the antimicrobial activities of future MTN inhibitors.

TABLE OF CONTENTS

DEDICATION	iv
ACKNOWLEDGEMENTS	v
ABSTRACT	vi
LIST OF TABLES	x
LIST OF FIGURES	xi
LIST OF ABBREVIATIONS.....	xiii
CHAPTER ONE: INTRODUCTION.....	1
S-adenosylmethionine Reactions	2
Methylthioadenosine/S-adenosylhomocystiene Nucleosidase and the Methionine Salvage Pathway	7
Quorum Sensing.....	13
Biofilms.....	17
<i>Escherichia coli</i> O157:H7.....	19
Metabolics and Proteomics of <i>E. coli</i> RK4353.....	25
Summary	28
CHAPTER TWO: MATERIALS AND METHODS	30
Creation of Electrocompetent Cells	30
Generation of the MTN Knockout (MTN KO) Strain Using the λ -Red System	30
Generation of the MTN Knock-In (MTN KI) Strain	32
Analysis of MTN Activity: Preparation of Bacterial Lysates.....	32

Analysis of MTN Activity: Immunoblot Assay.....	32
Analysis of MTN Activity: Enzyme Assay	33
Cell Growth Assays	33
Biofilm Assays.....	34
Adherence Assays.....	35
Vero Cell Cytotoxicity Assay	37
Type III Secretion System Protein Assay	38
Hemolysin Assays.....	39
Metabolic Enzyme Analysis	40
CHAPTER THREE: RESULTS AND DISCUSSION.....	42
Creation and Analysis of a Genetic MTN Knockout in <i>E. coli</i> O157:H7	42
Effect of MTN Deficiency on Growth.....	44
Effect of MTN Deficiency on Biofilms	47
Effect of MTN Deficiency on Virulence Factors	50
Adherence	50
Shiga Toxin.....	53
Type III Secretion System Proteins	55
Hemolysin.....	56
Metabolic and Proteomic Analysis of <i>E. coli</i> RK4353.....	58
Future Work	62
CHAPTER FOUR: CONCLUSION.....	63
REFERENCES	65

LIST OF TABLES

Table 1	Bacterial Autoinducers.....	15
Table 2	Autoinducer-2 Induced Effects.....	16
Table 3	Virulence factors affected by AI-2 in <i>E. coli</i>	24
Table 4	Proteomic Differences in the WT and KO strains of <i>E. coli</i> RK4353.....	60

LIST OF FIGURES

Figure 1.	S-adenosylmethionine metabolic reactions.....	3
Figure 2.	Synthesis of SAM.....	4
Figure 3.	SAM-dependent methyltransferase reaction	4
Figure 4.	Polyamine synthesis.....	5
Figure 5.	Autoinducer-1 synthesis.....	5
Figure 6.	Radical SAM reaction.....	6
Figure 7.	Structure of the <i>E. coli</i> Methylthioadenosine/S-adenosylhomocysteine Nucleosidase	8
Figure 8.	The methionine salvage pathway in bacteria.....	9
Figure 9.	Autoinducer-2 synthesis.....	10
Figure 10.	Early and late transition state analogues for MTN	12
Figure 11.	General scheme of a quorum sensing system	14
Figure 12.	Biofilm maturation is a complex developmental process involving five stages.....	18
Figure 13.	Model for the receptor mediated endocytic entry of Shiga toxin and processing of Shiga toxin in a mammalian cell	21
Figure 14.	A schematic of type III secretion structures in <i>E. coli</i> O157:H7	23
Figure 15.	Model for <i>luxS</i> -dependent quorum sensing in enterohemorrhagic (EHEC) and enteropathogenic (EPEC) <i>Escherichia coli</i>	25
Figure 16.	Central carbon metabolism with highlighted aspects affected by MTN deficiency	27
Figure 17.	Analysis of the <i>E. coli</i> O157:H7 MTN knock-out strain.....	43

Figure 18.	Comparison of growth of <i>E. coli</i> O157:H7 WT, MTN KO and MTN KI in Davis minimal media	45
Figure 19.	Comparison of biofilm production by <i>E. coli</i> O157:H7 WT and MTN KO strains	48
Figure 20.	Confocal microscopy of biofilms produced by <i>E. coli</i> O157:H7 WT, MTN KO and MTN KI strains	49
Figure 21.	Analysis of <i>E. coli</i> O157:H7 WT and MTN KO strain adherence to bovine Mac-T cells	52
Figure 22.	Effect of MTN deficiency on Shiga toxin production in <i>E. coli</i> O157:H7	54
Figure 23.	Comparison of virulence factor production in <i>E. coli</i> O157:H7 WT, MTN KO, and MTN KI strains	57
Figure 24.	Analyses of the specific activities of enzymes affected by MTN deficiency in <i>E. coli</i> RK3453	61

LIST OF ABBREVIATIONS

5'dADO	5' Deoxyadenosine
5-dRIB	5-Deoxy-D-Ribose
α -KDHC	α -Ketoglutarate Dehydrogenase Complex
ACP	Acyl Carrier Protein
ADH	Alcohol Dehydrogenase
AdoMet	S-adenosylmethionine
A/E	Attaching and Effacing Lesion
AHL	N-Acyl homoserine lactone
AI	Autoinducer
AI-1	Autoinducer-1
AI-2	Autoinducer-2
AI-3	Autoinducer-3
AIP	Autoinducer peptides
AMP	Adenosine Monophosphate
Amp ^r	Ampicillin Resistant
ATP	Adenosine triphosphate

BioB	Biotin Synthase
BSA	Bovine Serum Albumin
bp	Base Pair
CFU	Colony forming units
Cm ^r	Chloramphenicol Resistant
CoA	Coenzyme A
CRE	Carbenapem Resistant <i>Enterobacteriaceae</i>
DMEM	Dulbecco's Modified Eagle Medium
DMMG	Davis Minimal Media with 0.2% Glucose
DNA	Deoxyribonucleic acid
DI	Deionized
DPD	4,5-dihydroxy-2,3-pentanedione
DTT	Dithiothreitol
EHEC	Enterohemorrhagic <i>Escherichia coli</i>
ELISA	Enzyme-Linked Immunoabsorbent Assay
EPEC	Enteropathogenic <i>Escherichia coli</i>
Esp	<i>Escherichia</i> Secretion Protein
EspA	<i>Escherichia</i> Secretion Protein A
EspB	<i>Escherichia</i> Secretion Protein B

FBS	Fetal Bovine Serum
Gb3	Globotriaosylceramide
GDH	Glutamate Dehydrogenase
HC	Hemorrhagic colitis
HRP	Horseradish Peroxidase
HUS	Hemolytic Uremic Syndrome
IgG	Immunoglobulin G
IPTG	Isopropyl β -D-1-thiogalactopyranoside
KDH	α -Ketoglutarate Dehydrogenase
KI	Knock-in
KO	Knockout
LB	Luria Bertani Broth
LCMS	Liquid Chromatography-Tandem Mass Spectrometry
LDH	Lactate Dehydrogenase
LEE	Locus of Enterocyte Effacement
LipA	Lipoyl Synthase
LSM	Laser Scanning Microscopy
MAT	Methionine Adenosyltransferase
MOI	Multiplicity of Infection

MRSA	Methicillin resistant <i>Staphylococcus aureus</i>
MTA	5'-Methylthioadenosine
MTN	5'-Methylthioadenosine/S-adenosylhomocysteine nucleosidase
MTR	5-Methylthioribose
MTR-1-P	Methylthioribose-1-phosphate
MTP	Methylthioadenosine Phosphorylase
MTT	3-(4,5-Dimethylthiazol-2-yl)-2,5-diphenyltetrazolium bromide
NADH	Nicotinamide Adenine Dinucleotide
OD	Optical Density
PBS	Phosphate Buffered Saline
PBST	Phosphate Buffered Saline Tween
PCR	Polymerase Chain Reaction
PDH	Pyruvate Dehydrogenase
PDHC	Pyruvate Dehydrogenase Complex
PES	Phenazine Ethosulfate
pO157	Plasmid O157:H7
QS	Quorum-sensing
QseA	Quorum-sensing <i>E. coli</i> Regulator A
QseB	Quorum-sensing <i>E. coli</i> Regulator B

QseC	Quorum-sensing <i>E. coli</i> Regulator C
RNA	Ribonucleic acid
RPM	Revolutions per minute
SAH	S-Adenosylhomocysteine
SAM	S-Adenosylmethionine
SDS PAGE	Sodium Dodecyl Sulfate Polyacrylamide Gel Electrophoresis
SOC	Super Optimal Citrate Broth
SRBC	Sheep Red Blood Cell
SRH	S-ribosylhomocysteine
Stx	Shiga toxin
Stx-1	Shiga Toxin 1
Stx-2	Shiga toxin 2
ThiH	Tyrosine Lyase
Tir	Translocated Intimin Receptor
TRITC	Tetramethyl Rhodamine Iso-thiocyanate
tRNA	Transfer Ribonucleic Acid
TTSS	Type Three Secretion System
WT	Wild Type

CHAPTER ONE: INTRODUCTION

The development of antibiotics in the 19th century revolutionized the field of medicine by dramatically improving the ability to treat life-threatening infections. Paul Erlich, who would become known as the “Father of Antibiotics,” first hypothesized that if a dye was selectively toxic to bacterial cells, but not to mammalian cells, it would cure all infections.¹ After screening hundreds of dyes, Erlich discovered Salvarsan, the first synthetic antibiotic used specifically to treat syphilis. In 1929, Sir Alexander Fleming discovered that secreted products of the *Penicillium* mold could lyse *Staphylococcus* cells, which marked the first report of the antibacterial action of a natural fungal product.²

Subsequently, the first widespread introduction of effective sulfonamides by Domagk in 1937 was closely followed by reports of the development of bacterial resistance.³ Resistance to sulfonamides, originally reported in the late 1930s, persists today.² Bacterial resistance to penicillin was also reported by two members of the discovery team several years before its introduction as a therapeutic.⁴ Once penicillin was widely distributed in the 1940s and 1950s, drug-resistant strains expressing penicillinase (β -lactamase) activity became prevalent. To combat this, a widespread effort was made to develop synthetic penicillinase inhibitors and new generations of penicillin-based drugs that were resistant to earlier β lactamases.³ Invariably, the development and introduction of every antibiotic has been followed by eventual bacterial resistance.

A more startling trend is that many bacterial pathogens associated with epidemics of human disease have evolved multiple drug resistances.³ The evolution of drug

resistance is encouraged by the misuse of antibiotics and the rapid adaptability of bacteria. Hospitals serve as spawning grounds for many of these drug resistant strains. The most prevalent example is methicillin-resistant *Staphylococcus aureus* (MRSA), which developed resistance to methicillin only three years after the introduction of this drug.³ With time, MRSA acquired multiple forms of drug resistance and developed into a major community-acquired pathogen. Since then, a variety of other superbugs have emerged, including carbenapem resistant Enterobacteriaceae (CRE). As standard forms of antibiotics are becoming obsolete, there is a potential for all pathogenic bacteria to resist antibiotic treatment. Thus, there exists a dire need for novel forms of antibiotics to either replace or revitalize older drugs in order to prevent a reversion to the pre-antibiotic age when every infection was potentially life threatening.

S-adenosylmethionine Reactions

S-adenosylmethionine (SAM) is an important nucleoside found in all living organisms where it serves as an active group donor in a vast array of metabolic and biosynthetic reactions.⁵ The main use of SAM is as the primary methyl group donor in methylation reactions of macromolecules and small molecules. Other metabolic fates of SAM include the synthesis of acylhomoserine lactones (autoinducer-1, AI-1), polyamine synthesis (spermidine, spermine, etc), and radical SAM reactions involved in vitamin synthesis (Figure 1). SAM is synthesized in the cytosol by methionine adenosyltransferase (MAT), which joins L-methionine to ATP and yields SAM, pyrophosphate and phosphate ion (Figure 2).⁶ This transfer creates a metastable sulfonium ion, providing a target for nucleophilic substitution reactions that allow the transfer of methyl-, propylamino-, and other functional groups from SAM.

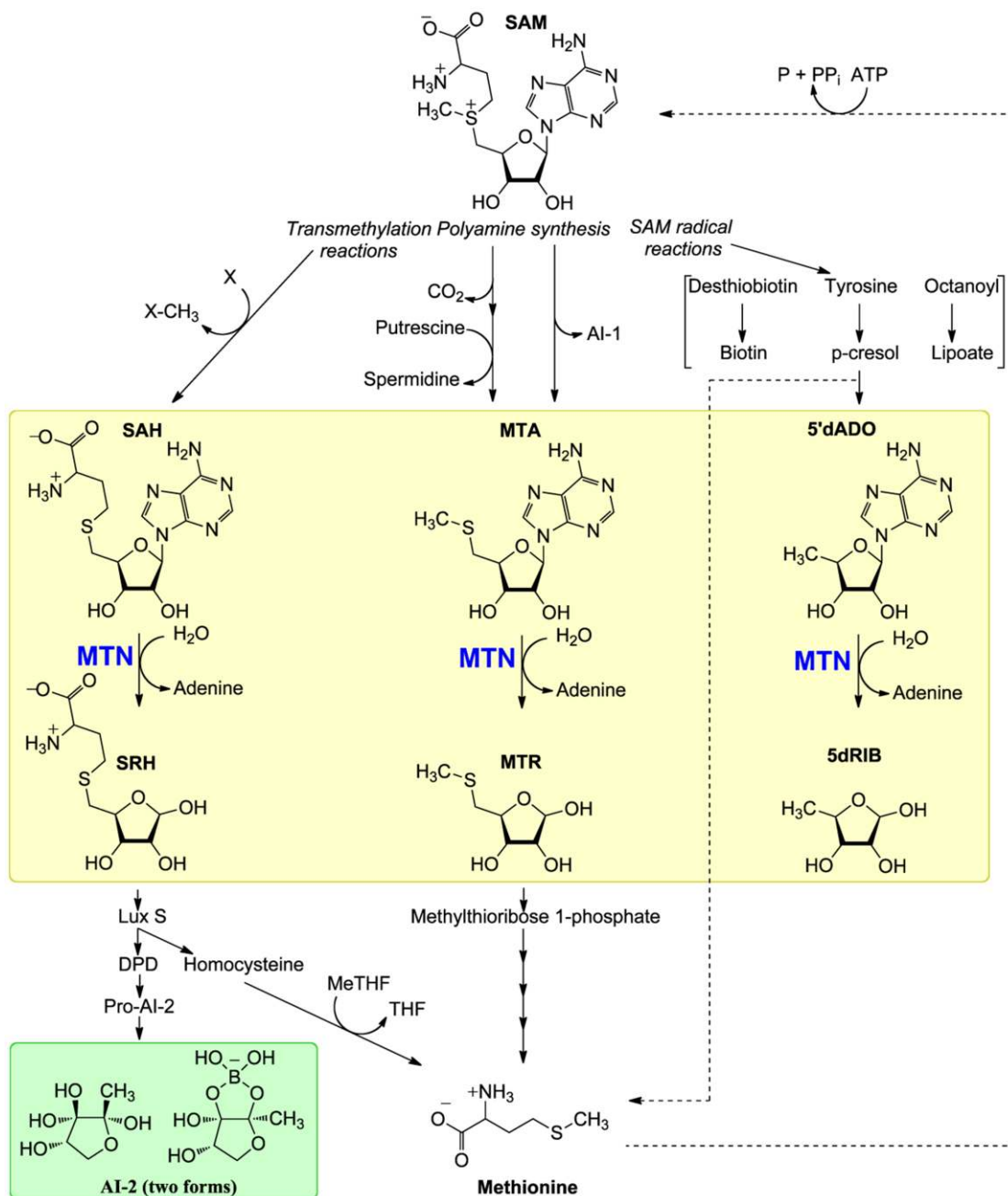


Figure 1. S-adenosylmethionine metabolic reactions. SAM is used as a reagent in transmethyations, polyamine synthesis, autoinducer synthesis, and radical SAM reactions. SAH, MTA, and 5'dADO are toxic side products of these reactions. MTN is responsible for the hydrolysis of the glycosidic linkage between the adenine and the ribose sugar. The ultimate goal of these reactions is to allow salvage of both methionine and adenine.

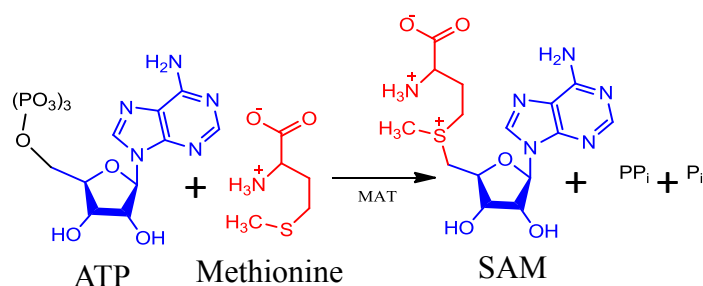


Figure 2. Synthesis of SAM. SAM is synthesized in the cytosol by methionine adenosyltransferase (MAT), which joins L-methionine to ATP and yields SAM, pyrophosphate, and phosphate ion.

SAM-dependent methyltransferase reactions are diverse and critical for survival (Figure 3). As an example, the methylation of cytosine in DNA regulates a variety of mammalian gene activities, somatic inheritance, and cellular differentiation.⁷ In bacteria, methylations are responsible for regulation of many processes, including motility, gene expression, and the bacterial cell cycle.⁵ SAM is also the major methyl donor for proteins, phospholipids, carbohydrates, and various other molecules. While a variety of reaction mechanisms are used in transferases, the byproduct of all the reactions is S-adenosylhomocysteine (SAH).⁵

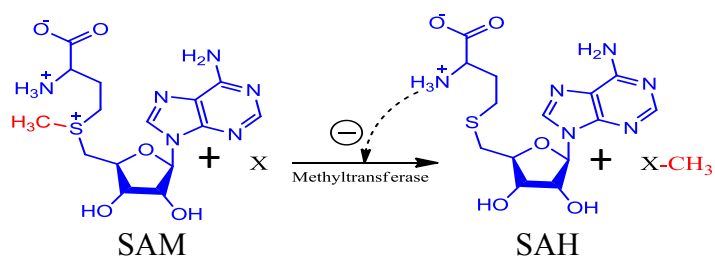


Figure 3. SAM-dependent methyltransferase reaction. Generic representation of SAM acting as a methyl donor. SAH can act as a product inhibitor to these reactions.

Polyamine and autoinducer syntheses are also SAM dependent and essential molecules for cell growth and communication. The byproduct in each reaction is methylthioadenosine (MTA). Spermidine is produced from the transfer of a 5'

propylamine group from decarboxylated SAM to putrescine by spermidine synthase (Figure 4).^{5,11} Polyamines are fully protonated under physiological conditions and thus carry a positive charge that form ionic interactions with negatively charged nucleic acids, specific proteins, and phospholipids.¹¹ It is known that the rate of DNA synthesis is decreased by polyamine deficiency. Polyamines also confer protective effects against apoptosis, and play a major role in protein synthesis.¹¹

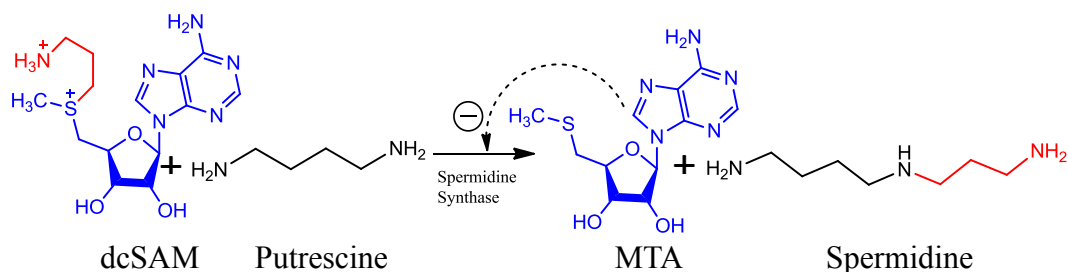


Figure 4. Polyamine synthesis. Spermidine synthase transfers the 5' propylamine group from decarboxylated SAM to putrescine to produce spermidine. MTA acts as a product inhibitor of this reaction.

N-acylhomoserine lactones (AI-1) are synthesized from the donation of an acyl group from hexanoyl acyl carrier protein (ACP) to SAM.⁵ In this reaction, a cyclization occurs to form the internal lactone ring and MTA as a byproduct (Figure 5).

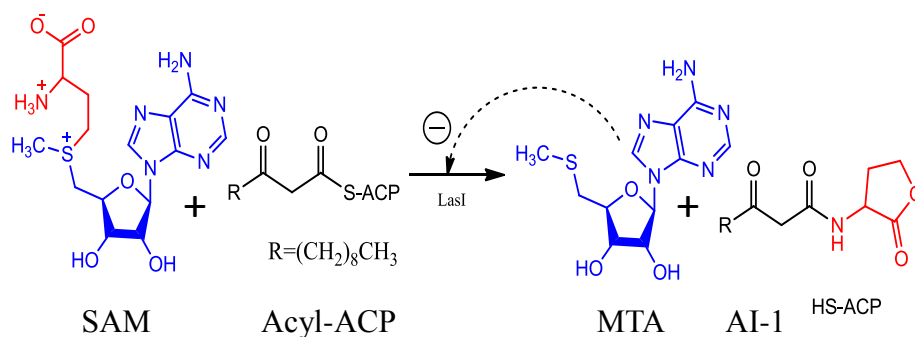


Figure 5. Autoinducer-1 synthesis. AI-1 is synthesized from the donation of an acyl group from hexanoyl ACP to SAM by LasI. MTA can act as a product inhibitor to this reaction.

SAM is also used as an oxidizing agent in radical SAM dependent reactions. The general reaction catalyzed by radical SAM enzymes occurs first by the reduction of the sulfonium by a coordinated iron-sulfur cluster.^{9,10} The newly formed radical abstracts a hydrogen from a substrate C-H bond (Figure 6).¹¹ Products of this abstraction vary greatly and include anaerobic oxidations, sulfur insertions, isomerizations, ring formation, and unusual methylations.⁵ In addition to the formation of the desired product, methionine and 5'-deoxyadenosine (5'-dADO) are formed as byproducts that can be recycled back to form SAM.

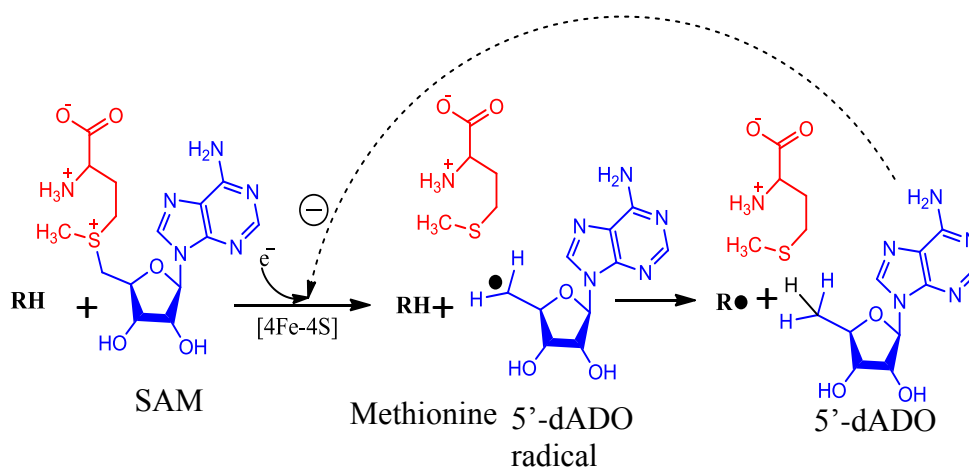


Figure 6. Radical SAM reaction. Reduction of the sulfonium occurs through coordination to an iron-sulfur cluster. The radical abstracts a hydrogen from a substrate C-H bond. Methionine and 5'-dADO are formed as byproducts. 5'-dADO can act as a product inhibitor to this reaction.

Radical SAM reactions are important to the synthesis of secondary metabolites, vitamins, antibiotics, and assist with bacterial DNA repair. Biotin synthase is a radical SAM enzyme that catalyzes the substitution of a bridging sulfur atom for hydrogen in desthiobiotin to form the essential enzyme cofactor biotin.¹² Lipoyl synthase is another radical SAM enzyme that catalyzes the final step in *de novo* biosynthesis of the lipoyl cofactor by inserting two sulfur atoms into an 8-carbon-saturated fatty acyl chain.¹⁴

Precursors of the cofactor thiamine are generated in several bacteria by the enzyme tyrosine lyase, a radical SAM enzyme.¹³ Overall, the radical SAM super family is currently composed of more than 2800 proteins involved in over 40 distinct biochemical transformations.⁸

A regulatory characteristic of all of the above SAM dependent reactions is the susceptibility to product inhibition by SAH, MTA, and 5'-dADO.⁵ SAH has been shown *in vitro* to inhibit a number of bacterial methyltransferases at low micromolar concentrations.^{15,16} Several reports have also shown that enzymatic degradation of SAH by MTA/SAH nucleosidase alleviates product inhibition of methylation reactions.^{17,18} The nucleoside MTA has also been shown to be a potent inhibitor of polyamine synthase reactions at low micromolar concentrations.¹⁹⁻²¹ In addition, MTA inhibits 50% of autoinducer-1 synthase activity at concentrations as low as 5 μ M.²¹ Lastly, 5'-dADO and methionine were shown to inhibit biotin synthase, lipoyl synthase, and tyrosine lyase.¹⁰ In order to reduce product inhibition by these nucleosides, all organisms have developed efficient nucleosidases to catabolize them and salvage their constituent parts.

Methylthioadenosine/S-adenosylhomocystiene Nucleosidase and the Methionine Salvage Pathway

Methylthioadenosine/S-adenosylhomocysteine nucleosidase (MTN) catalyzes the irreversible cleavage of MTA, SAH, and 5'-dADO to adenine and the corresponding pentose, 5-methylthioribose (MTR), S-ribosylhomocysteine (SRH), and 5-deoxy-D-ribose (5-dRIB), respectively.^{5,22} MTN exists as a 25-35 kD homodimer and is found in the methionine salvage pathway for the majority of bacteria (Figure 7).^{5,22,24} Specifically in 51 bacterial species, including pathogens with reductive genomic evolution, MTN is

responsible for metabolism of the three nucleotides.^{23,25} Other bacteria that contain relatively large genomes and exhibit complex metabolism use two enzymes to remove MTA and SAH independently.²⁶ These organisms behave metabolically more like humans: a MTA phosphorylase converts MTA to 5-methylthioribose-1-phosphate, while SAH hydrolase catabolizes SAH.⁵ This more restricted substrate specificity is proposed to allow more efficient metabolism to promote better survival in these organisms.^{27,28}

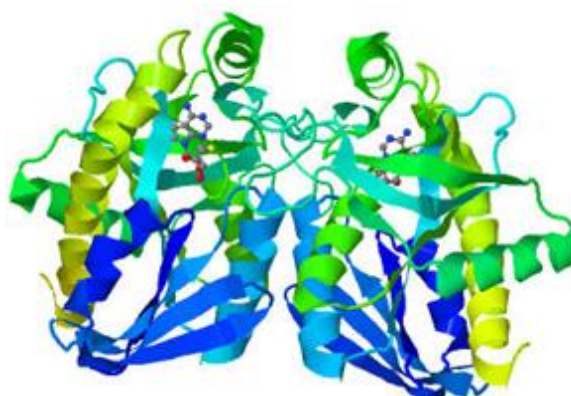


Figure 7. Structure of the *E. coli* Methylthioadenosine/S-adenosylhomocysteine Nucleosidase. Ribbon representation of the *E. coli* MTN dimer viewed down the noncrystallographic two-fold axis. A molecule of the MTA analogue Formycin-A is shown bound in each active site. (adapted from Lee et al., 2001)²³

The ultimate purpose of MTN is to catabolize growth inhibitory MTA, SAH, and 5'-dADO; and salvage the methionine and adenine, which are metabolically expensive to synthesize.⁵ The adenine is recycled back to purine nucleosides. The thiopentoses MTR and SRH require further enzymatic reactions to salvage the sulfur atom back into methionine (Figure 8).^{5,29,30} The conversion of MTR to methionine begins with the phosphorylation of MTR to MTR-1-phosphate (MTR-1-P) by MTR kinase.²⁹ In bacteria that contain a complete salvage pathway, an additional four or five enzymatic steps (depending on the species) are required to convert MTR-1-P to methionine.⁵ Some

organisms such as *E. coli*, that live in sulfur rich environments do not salvage methionine and secrete MTR, instead.³²

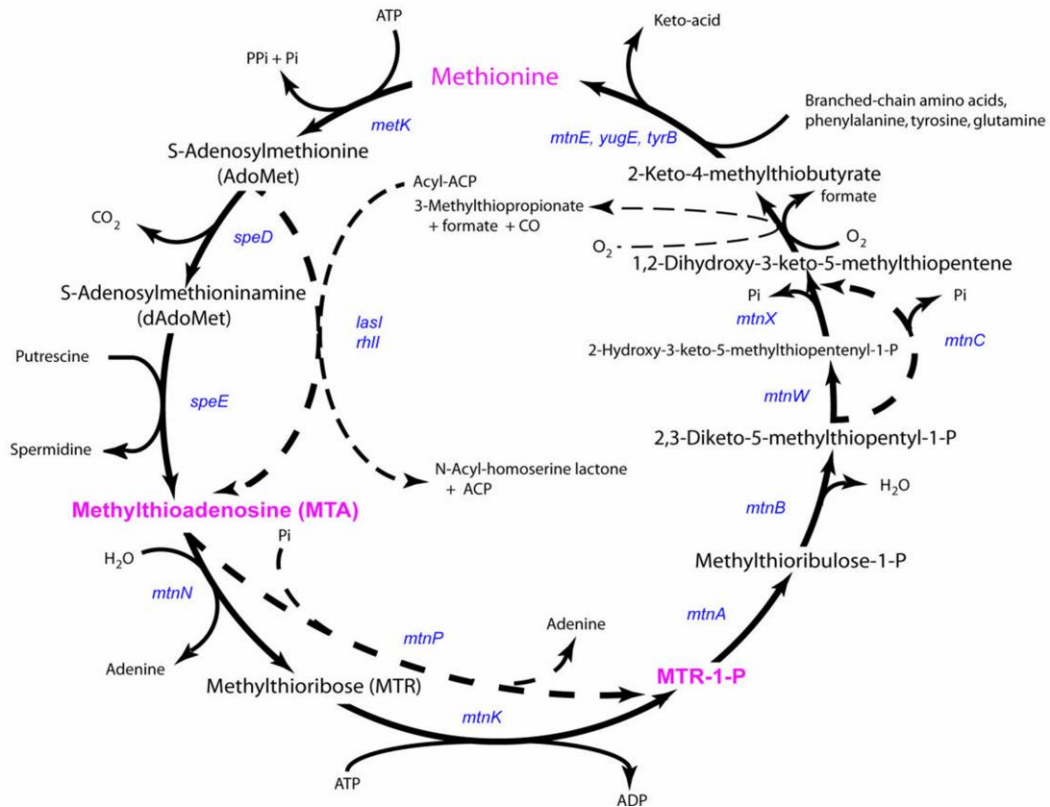


Figure 8. The methionine salvage pathway in bacteria. Dashed lines represent species variations. (adapted from Sekowska et al., 2004).²⁵

To salvage methionine from SAH catabolism, the majority of bacteria use the enzyme LuxS to cleave the thiopentose S-ribosylhomocysteine (SRH) to produce homocysteine and 4,5-dihydroxy-2,3-pentadione, the precursor to autoinducer-2 (AI-2, Figure 9).⁵ Homocysteine is remethylated to form methionine using either cobalamin-dependent (MetH) or cobalamin-independent (MetE) methionine synthases.^{33,68}

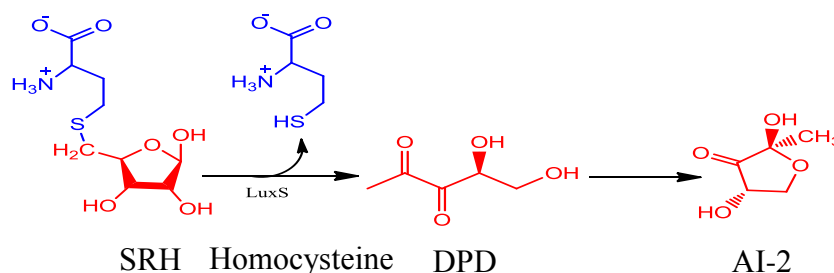


Figure 9. Autoinducer-2 synthesis. LuxS cleaves SRH to produce homocysteine and 4,5-dihydroxy-2,3-pentadione, which can then cyclize to form AI-2.

MTN is a potential novel antibiotic target due to its critical involvement in microbial metabolism and its absence in humans. The first description of MTN enzyme activity was reported in 1963.⁸⁹ In 1979, a study of MTA analogs was published that demonstrated that they were effective competitive inhibitors of MTN, and set the stage for further exploration of this enzyme as a chemotherapeutic target.³⁴ This initial discovery led to further studies on the development of substrate and transition-state analogs.^{31,39,40} Extensive crystallographic studies revealed MTN exists as a homodimer and established that enzyme-substrate interactions responsible for recognition and catalysis.³⁵⁻⁴⁰ Importantly, these studies revealed that the active site of each subunit contains a hydrophobic pocket involved in recognition of the 5' alkyl portion of the nucleoside that is partially composed of residues from the second subunit.^{22,34-37} The hydrolysis of the substrates is essentially irreversible and the acidic amino acid residues, Glu¹², Glu¹⁷⁴, and Asp¹⁹⁷, involved in catalysis are highly conserved across species.^{25,36,37}

While substrates and transition states are similar between bacterial MTN and mammalian MTA phosphorylase (MTP), crystallographic studies also reveal distinct differences in the enzyme active sites. In MTN, the active site has a larger 5' alkylthio binding pocket, which allows for recognition of SAH and other larger thionucleoside analogues than the active site of MTP.³⁵ There are also surface charge differences in the

region of the enzymes responsible for recognition of the 2'hydroxyl-group on the nucleoside: MTP is positively charged, while MTN is negatively charged.³⁵ Combined, these features suggest routes for directed drug design that would yield inhibitors capable of discriminating between the two enzymes.⁵ The majority of the work to develop specific selective inhibitors of MTN has been performed in Dr. Vern Schramm's lab at Albert Einstein College.^{31,38-40,71} These inhibitors are based on transition state structures for the substrate that would bind the enzyme active site with the highest affinity. Recent specific potent late transition stage MTA analogs with bulky 5' substitutions (DADMe-immucillin 54: DADMe-immucillin 57) are selective inhibitors that bind with a thousand-fold greater affinity (or more) to MTN than to MTP (Figure 10).³⁸⁻⁴⁰ However, most of the studies testing MTN transition state inhibitors as antibiotics in *E. coli* and other bacterial species have reported only modest activity, with IC₅₀ values in the micromolar range or higher.⁵ It has been proposed that the transition state analogs failed to exert potent antibiotic effects due to poor drug permeability or transport into the cell.³⁹ However, in species that are purine auxotrophs, such as *Borrelia burgdorferi*, MTN inhibitors were more potent.⁴⁰ Probably this is due to the greater need by these organisms to salvage methionine and purines, which makes them more sensitive to MTN interruption.⁴⁰

Despite rather poor antibiotic effects in *E. coli*, MTN transition state analogues have been shown to reduce AI-2 synthesis and biofilm formation.³⁹ Thus, the inhibitors have been proposed to act more as interrupters of microbial autoinducer signaling than as direct bactericidal agents. This may be critically important since virulence, pathogenesis, and drug resistance are thought to be regulated (at least partially) by intercellular

communication. Interruption of bacterial communication represents a new paradigm for the development of antibiotics. These drugs could act less directly than traditional antibiotics (like penicillin) to kill bacteria. Instead, they could cause attenuation of the pathogen so that the host immune system could more effectively combat the infection.

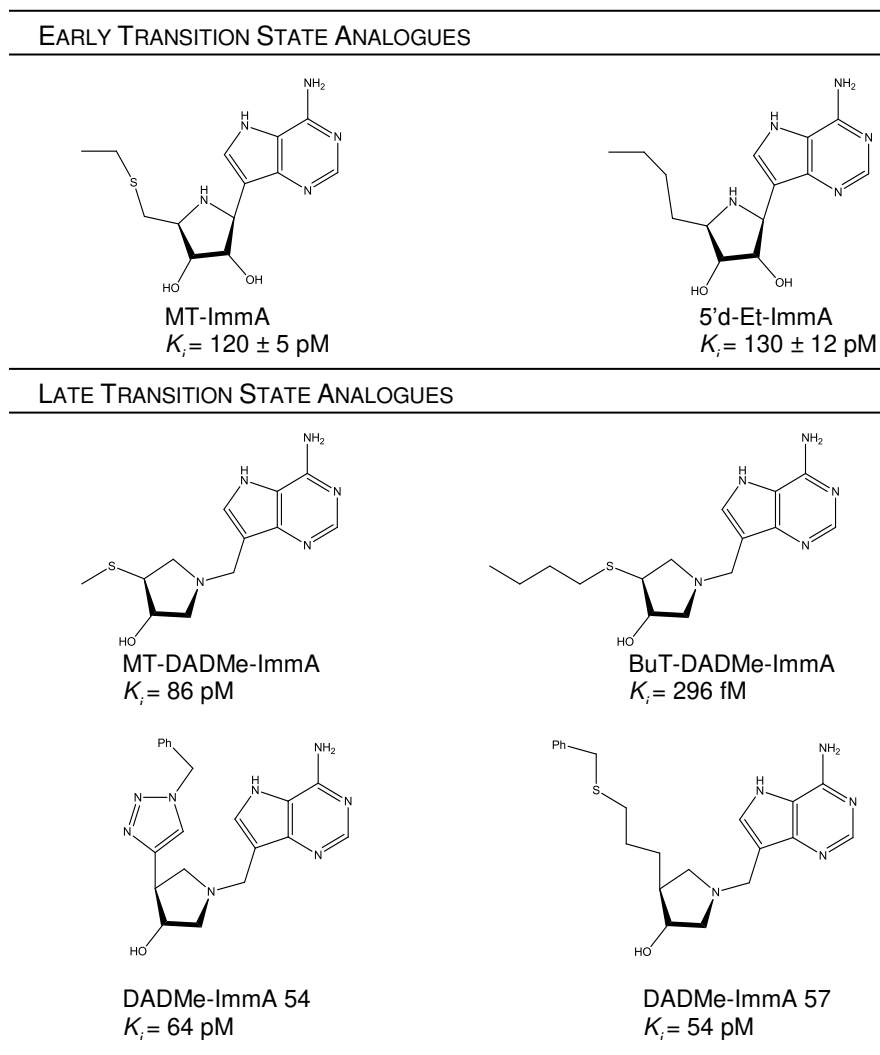


Figure 10. Early and late transition state analogues for MTN. Inhibitors of MTN contain a non-hydrolyzable linkage between the adenine and pentose moieties. The selectivity index for bacterial MTN can be up to a 1000 fold higher when compared to human MTP. All K_i values reported are for *E. coli* MTN and were obtained from the literature.^{31, 37-40, 71}

Quorum Sensing

Quorum sensing (QS) is the process of bacterial cell to cell communication that involves production, detection, and response to extracellular signaling molecules known as autoinducers (AI).⁴⁵ QS was originally discovered over 30 years ago in two bioluminescent bacterial species, *Vibrio fischeri* and *Vibrio harveyi*. In these species, light emission occurred only at high cell population density, when the accumulation of secreted AIs stimulated the expression of the structural operon *luxCDABE*, which encodes the light producing luciferase enzyme.⁴⁵ Since this initial discovery, it has been reported that QS is responsible for an array of bacterial phenotypes and behaviors including sporulation, competence, antibiotic production, biofilm formation, and virulence factor secretion.⁴⁵

While the regulatory components and molecular mechanisms of QS differ between bacterial species, three basic principles apply. First, all communicating bacteria produce AIs. When the population of a bacterial community is low, the AIs are in such low concentration that they are unable to stimulate a population-wide response. After the population reaches a high density, the additive amount of AIs produces a cumulative response. The second principle of QS is that receptors for AIs exist in the membrane or the cytoplasm of the responding cells. Lastly, AIs induce varied gene expression and stimulate production of additional AIs through a positive feedback loop to sponsor synchronous behavior in the cell population (Figure 11).⁴⁵

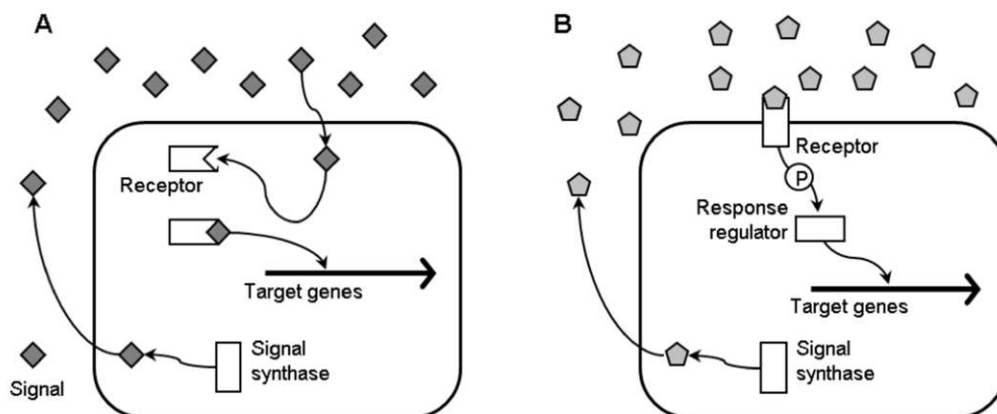
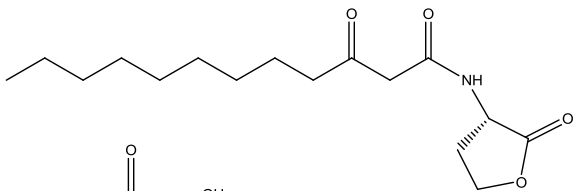
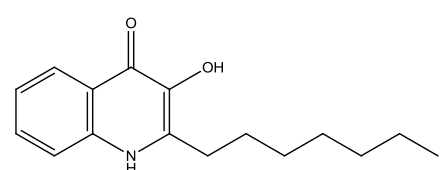
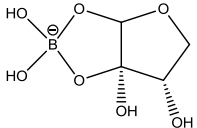
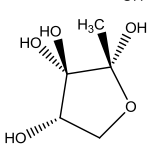
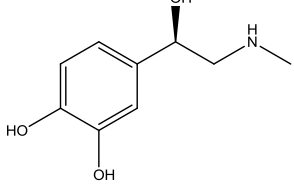
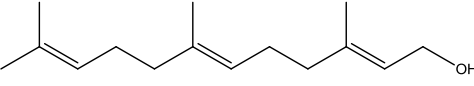
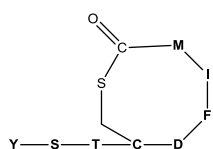


Figure 11. General scheme of a quorum sensing system. The signal synthase enzyme produces signal molecules, which reach the extracellular environment via diffusion or transport. At a critical signal molecule concentration, the signal binds to the receptor, which can be located in the cytoplasm (A) or at the cell surface (B). If the receptor is located in the cytoplasm, the signal-receptor complex activates or inactivates transcription of target genes. If the receptor is located at the cell surface, the signal sets off a phosphorylation signal transduction cascade that activates a transcriptional regulator at the end modulate target gene transcription. (adapted from Defoirdt et al., 2010).⁹⁷

The mechanism of QS differs in Gram-positive and Gram-negative bacteria. In Gram-positive bacteria, small cyclic peptides (AIP) are used as signaling molecules while in Gram-negative bacteria small molecules such as acyl-homoserine lactones are used (Table 1). *Staphylococcus aureus*, a Gram-positive pathogen, utilizes AIPs to regulate the *agr* system that controls over 70 genes. Many of these genes code for known virulence factors.⁸⁷ The first class of small molecule AIs (AI-1) is primarily used for intraspecies communication in Gram-negative bacteria. AI-1 synthases use SAM as a substrate to produce a variety of acylhomoserine lactones (Table 1), with MTA as a byproduct. *Pseudomonas aeruginosa* utilizes AI-1 to regulate the production of several extracellular virulence factors, promote biofilm maturation, and regulate the expression of antibiotic efflux pumps.⁵¹

Table 1. Bacterial Autoinducers

Autoinducer Type	Autoinducer Molecule
AI-1	
AI-1	
AI-2	
AI-2	
AI-3	
Farnesol	
AIP	

The second class of small molecule AIs (AI-2) is considered a “universal” signaling molecule that allows inter-species communication.⁴⁶⁻⁴⁸ AI-2 is produced by the enzyme LuxS, which synthesizes 4,5-dihydroxy-2,3-pentanedione (DPD) that spontaneously cyclizes into a pro-AI-2 structure (Figure 9).^{48,49} In marine environments where boron is plentiful, pro-AI-2 spontaneously forms a boron diester structure (Table 1).^{46,47,49} However, a large number of bacterial species synthesize and respond to AI-2 in environments that may not contain boron, other derivatives of DPD exist. For some

species, the formation of DPD is purely a byproduct of metabolism.⁴⁷ AI-2 has been shown to regulate biofilms and virulence factors in *E. coli*, as well as various other species (Table 2).^{51, 76}

Table 2. Autoinducer-2 Induced Effects

Phenotype	Bacterium
Biofilms	<i>E. coli</i> , <i>Helicobacter pylori</i> , <i>Pseudomonas gingivalis</i> , <i>Streptococcus gordonii</i> , <i>Streptococcus mutans</i>
Virulence Factors	<i>Clostridium perfringens</i> , <i>E. coli</i> , <i>Neisseria meningitidis</i> , <i>Pseudomonas gingivalis</i> , <i>Serratia marcescens</i> , <i>Streptococcus pyogenes</i> , <i>Vibrio cholerae</i>
Bioluminescence	<i>Vibrio fischerii</i> , <i>Vibrio harveyi</i>

There have been extensive investigations on the effects of *luxS* gene deletions, due to its direct connection with quorum sensing. *Neisseria meningitidis luxS* knockout strains were found to have reduced virulence.⁴⁴ In other studies, *luxS* deficiency was found to alter sporulation in *Bacillus subtilis*, hemolysin secretion in *Listeria monocytogenes*, and twitching motility involved in colonization and biofilms in *E. coli* and *Salmonella*.⁹²

An expanding list of other autoinducers has also been described. This includes autoinducer (AI-3), a molecule that is reported to have an epinephrine-like structure and may allow the bacteria to respond to host signaling molecules. In *E. coli* 0157:H7, AI-3 appears to regulate the formation of attaching and effacing lesions.^{67,86} Lastly, microbial intercellular communication is not confined to bacteria, the isoprenoid farnesol is reported to act as an AI in the yeast *Candida albicans*.⁸⁸

Biofilms

In nature, the majority of bacteria are found within biofilms. Biofilms are composed of communities of bacterial cells that attach and proliferate on living or nonliving surfaces using a secreted extracellular polysaccharide matrix.⁵³ This adhered communal existence allows bacteria to occupy a favorable microenvironment rather than simply being randomly dispersed. Thus, the traditional view of bacteria as existing solely as planktonic or free-swimming cells has now been replaced by the idea that the planktonic phase is simply a mechanism for translocation from one surface to another.⁵² Many persistent and chronic bacterial infections are attributed to formation of biofilms in wound sites or on medical implants that resist antibiotic treatment and evade host immune responses.⁵⁴ In addition, bacterial biofilms on food processing equipment and surfaces are a leading cause of food-borne illness.⁵³

Biofilm formation is a sequential process (Figure 12). In the first phase, the planktonic bacterial cells form a transient association with a new surface or to previously adhered microbes. Upon finding a suitable location, the bacteria progress from a transient association to form a microcolony. This colony may consist of one species or (more commonly) a heterogenous mix of species. At this stage, the cell density reaches levels that quorum sensing through AI molecules becomes feasible. The QS signaling pathways lead to altered gene transcription that stimulates production of an exopolysaccharide matrix that envelopes the micro-colony. Further alteration of gene transcription occurs to adapt the individual bacterial cell to communal existence within the biofilm. The modulation of biofilm unique genes includes the up-regulation of a wide array of enzymes and transporters, such as adaptive surface enzymes used to metabolize the chitin

from insects and crustaceans, and the creation of specialized nutrient transport channels within the matrix.^{52,53} In multispecies biofilms, bacteria establish micro-communities within the matrix that are optimized for both survival and symbiotic relationships between the groups of bacteria.⁵³ In essence, a biofilm is not a random assortment of bacteria, but more akin to a developed city with defined architectures that allow a variety of optimal microenvironments to exist.

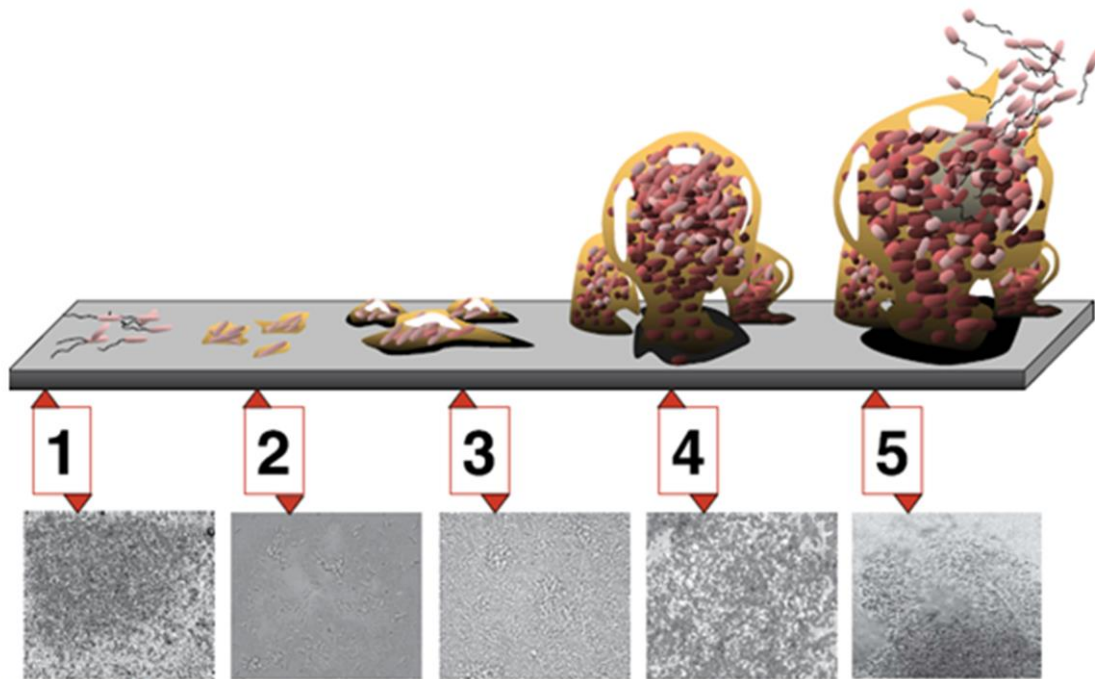


Figure 12. Biofilm maturation is a complex developmental process involving five stages. Stage 1: initial attachment; stage 2: irreversible attachment; stage 3: maturation I; stage 4: maturation II; stage 5: dispersion. Each stage of development in the diagram is paired with a photomicrograph of a developing *P. aeruginosa* biofilm. (adapted from Monroe, 2007).⁸⁴

Biofilms pose a major concern for the treatment of bacterial infections. The extrapolymeric matrix provides a shield against bacteriophages and amoebae, attenuates responses to antibiotics, and decreases access by the host immune system.^{54,55} The thickness of the biofilm matrix prevents antimicrobial agent penetration to the full

depth required to eliminate all of the microbes, and hinders phagocytosis by host neutrophils. Ultimately, this allows planktonic cells to escape and form other foci of infection^{54,55} Since traditional antibiotics work to both eradicate pathogens and support host immune responses, these are much less effective in the context of biofilms.

***Escherichia coli* O157:H7**

Enterohemorrhagic *Escherichia coli* O157:H7 is a pathogen often associated with foodborne illness. Infection can lead to devastating or life-threatening systemic manifestations such as hemolytic uremic syndrome (HUS) and hemorrhagic colitis (HC).⁵⁶ The main cause of these serious ailments originates from the release of bacterial Shiga toxins (Stxs) during the infection, and subsequent damage to cells in the intestines, kidneys, brain, and other organs.⁵⁶ While other serogroups of *E. coli* also produce Stxs, and are often more prevalent in humans, *E. coli* O157:H7 is especially virulent and responsible for the majority of HUS cases worldwide.^{56,57}

E. coli O157:H7 was first recognized in 1982 when an outbreak associated with contaminated hamburger occurred in the Jack-in-the-Box restaurant chain in Oregon and Michigan.⁵⁸ Since then, sporadic outbreaks have occurred throughout the world. In 1998, a particularly large outbreak occurred in Japan, when over 9,000 children were infected.⁵⁹

Symptoms of infection begin with severe cramps, initially followed by watery and then bloody diarrhea, with little or no fever.⁶⁰ About 10% of cases develop into HUS, which carries a mortality rate of 2-10%.⁵⁷ The most susceptible to the development of HUS are young children and the elderly.⁶⁰

The three principal routes of transmission are: fecal-contaminated food and water, person-to-person spread, and animal contact.⁶⁰ The major animal carriers are healthy

cattle, and to a lesser degree other domesticated ruminants like sheep and goats.⁵⁶ These animals act as reservoirs. *E. coli* O157:H7 is distributed through feces, which can contaminate foods when manure is used as a fertilizer or by direct contact during the slaughter and preparation of meat. Of these, contaminated meat, unpasteurized milk, and fecal-contaminated fruit and vegetables are the most common vehicles of transmission. However, undercooked ground beef is the major source of transmission accounting for 75 out of 183 reported foodborne outbreaks in the US between 1982 and 2002.⁵⁷

The production of two antigenically distinct forms of Stx (Stx1 and Stx2) by *E. coli* O157:H7 results in HUS and HC.⁶¹ Both toxins are compound toxins consisting of a catalytic A subunit and a cell targeting pentameric B subunit.^{56,57} After entering the cell through receptor mediated endocytosis, the A subunit is proteolytically cleaved to yield the catalytically active RNA N-glycosidase. This enzyme cleaves specific bonds in the rRNA, preventing the binding of amino acyl-tRNA to the ribosome. This inhibits the elongation of the peptide chain during peptide synthesis and eventually leads to cell death (Figure 13).⁶¹ Ruminants lack the vascular Stx sensor, globotriaosylceramide. This allows them to act as *E. coli* O157:H7 carriers unaffected by Stx toxicity.⁵⁶

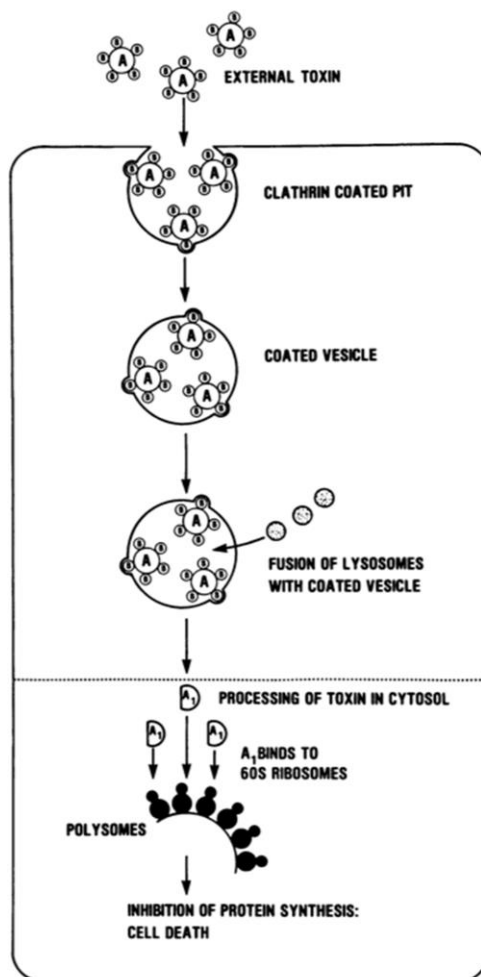


Figure 13: Model for receptor mediated endocytic entry and processing of Shiga toxin in a mammalian cell. Shiga toxin enters the cell by receptor-mediated endocytosis. The B subunit of the toxin binds to the mammalian cell receptor globotriaosylceramide (Gb3). The clathrin-coated pit is pinched off, and the coated vesicle is formed. The vesicle is acidified, and may fuse with lysosomes. The A₁ fragment within the cytosol binds the 60S ribosome, leading to inhibition of protein synthesis and cell death. (adapted from O'Brien et al., 1987).⁶¹

The ability of Stx to produce attaching and effacing (A/E) lesions on a variety of cell types is one of the most important virulence characteristics found in *E. coli* O157:H7. The A/E lesions can be described by degeneration and effacement of intestinal epithelial cell microvilli, intimate adherence of bacteria to the epithelial cell surface and bacterial

directed assembly of highly organized cytoskeletal structures in the host cells.⁵⁷ These organized cytoskeletal elements form pedestal-like structures beneath the adhered *E. coli* O157:H7 cells and are a hallmark of this type of infection. Genetic studies have shown that the genes responsible for A/E lesions map to a region that is designated the locus of enterocyte effacement (LEE), and are considered a chromosomal pathogenicity island.⁶⁶ LEE is composed of at least 41 different genes, all required for bacterial adherence to the host cell.

The mechanism of adherence to host cells is very complex and a multitude of factors play a role in the process. *E. coli* O157:H7, like many other Gram-negative bacteria, has a type III protein secretion system (TTSS), which is a complex surface structure used to deliver virulence proteins into the host cell (Figure 14).^{62,63} TTSS consists of a needle-like flagella that pierces the host cell to inject proteins that modify the membrane. The needle like flagella is comprised of multiple *Escherichia* secretion proteins (Esp) with EspA forming a filamentous structure on the bacterial surface that forms a bridge to the host cell; essentially the tip of the needle.⁶⁴ EspB and EspD are injected through the needle into the mammalian cell membrane, where they form the end of the translocation complex required for other larger virulence factors to be injected directly into the host cell cytoplasm.^{62, 63}

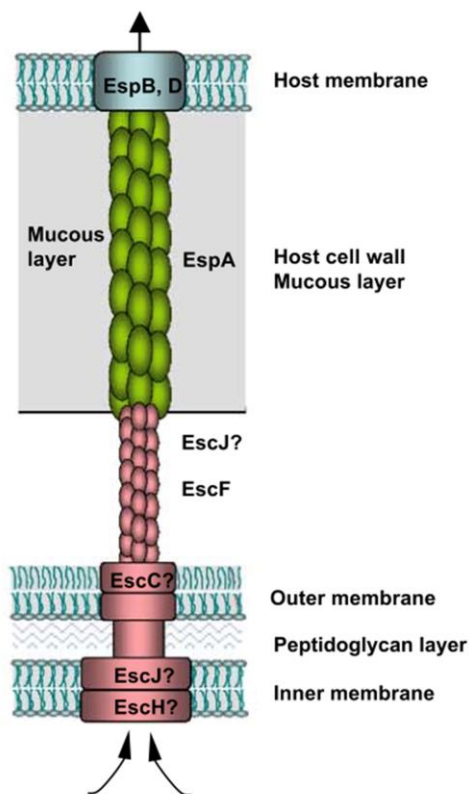


Figure 14: A schematic of type III secretion structures in *E. coli* O157:H7. Type III secretion structures are composed of a needle-like complex (pink), which is anchored in the bacterial cell wall and a translocation complex (blue) in the host membrane. EspA (in green) extends from the tip of the needle and penetrates the host mucous barrier and thick glycocalyx reaching the underlying intestinal enterocytes. (adapted from He et al., 2004.)⁶³

Adherence of *E. coli* O157:H7 to a mammalian cell is initiated by transfer of a translocated intimin receptor (Tir) into the host cell. Tir, much like EspB, becomes part of the mammalian cell membrane and provides a binding site for bacterial intimin. After this binding occurs, Tir links host actin fibers to the membrane to form the characteristic pedestal structure.⁶⁵ This intimate binding allows other virulence factors to wreak havoc on the host cell, eventually leading to A/E lesions.

The plasmid O157 (pO157) encodes for a myriad of additional virulence factors not found in the chromosomal DNA.⁶⁶ The first described virulence factor of pO157 was

hemolysin, an endotoxin that lyses red blood cells by destroying their cell membrane through phospholipase activity. While hemolysin is not essential for producing either HUS or HC, the lysis of red blood cells provides iron for the pathogen that stimulates growth and production of other toxins.⁵⁷ Other virulence factors encoded on pO157 are catalase-peroxidase, type II secretion proteins, serine protease, metalloprotease, and putative adhesion genes.⁶⁶

Virulence regulation in O157:H7 has been attributed to *luxS* mediated quorum sensing (Table 3).^{23,67} The transcriptional regulation of genes in the LEE initiated through quorum sensing is complex since it consists of two regulators and multiple gene operons (Figure 15).⁷⁵ The initial belief was that AI-2 controlled all aspects of virulence, but this was later disproved when *luxS* mutants were still able to produce A/E lesions in cultured epithelial cells.⁶⁷

Table 3. Virulence factors affected by AI-2 in *E. coli*

Virulence Factor	Ref
Biofilm production	52
Motility	86
<i>lee</i> operons	80
<i>qse</i> transcription	79
Type III secretion	80
Generation time	86
Gene expression (404 genes)	86

Further investigation determined that the genes for TTSS were AI-3 dependent, a signaling molecule that resembles epinephrine.⁶⁷ Bacterial AI-3 receptors can also bind host cell produced epinephrine, thus providing a link between mammalian and bacterial communication pathways. It remains unclear whether the other aspects of virulence such as toxin production and biofilm formation are AI-2 or AI-3 dependent.

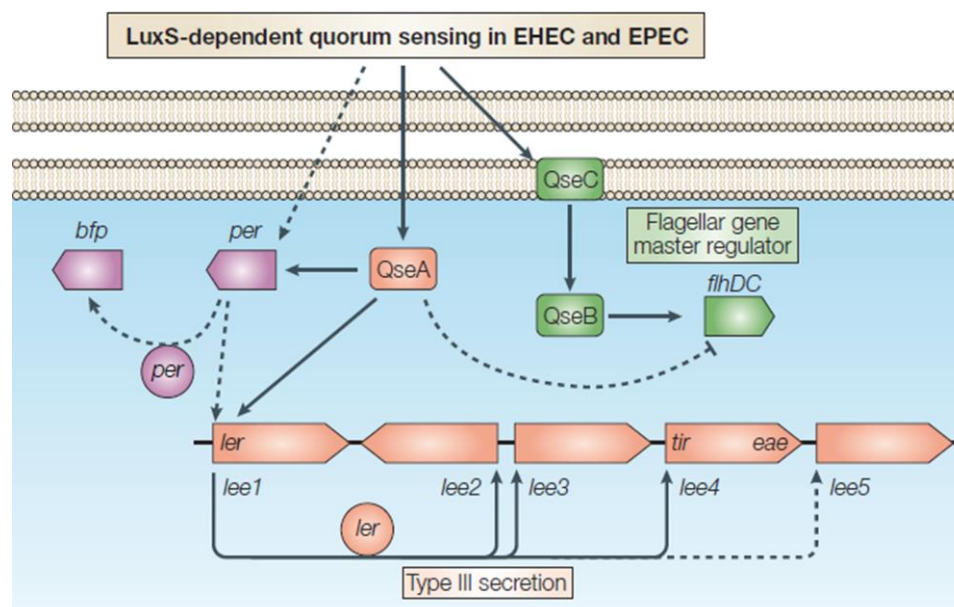


Figure 15. Model for *luxS*-dependent quorum sensing in enterohemorrhagic (EHEC) and enteropathogenic (EPEC) *Escherichia coli*. Interactions limited to EPEC are indicated by dashed lines. The histidine kinase QseC (quorum-sensing *E. coli* regulator C), together with its cognate response regulator QseB, activates the flagellar master operon *flhDC* (green boxes). Regulation of type III secretion (red boxes) is mediated through QseA, and indirectly through Ler. Together, the two proteins activate expression of five important *lee* operons that encode components of the type III secretion apparatus as well as adhesion proteins (intimin, Eae), the translocated intimin receptor (Tir), and other proteins. (adapted from Vendeville et al., 2005.)⁷⁶

Metabolomics and Proteomics of *E. coli* RK4353

In recent years, liquid chromatography-tandem mass spectrometry (LCMS) has become an invaluable tool for the analysis of bacterial organisms. Extensive metabolic and proteomic analysis have been performed on a plethora of bacterial species to understand basic metabolism, and the changes to metabolism that occur in response to drug treatment, gene deletion, and changes in environment.⁶⁹ This knowledge can be used to direct drug design by revealing new or additional targets.

A *pfs* (MTN) gene knock-out strain was originally created in *E. coli* RK4353 to investigate potential gene polarization effects that occurred when deleting the gene encoding the periplasmic cobalamin-binding protein.⁶⁸ While this Δpfs mutant was not created for the purpose of analyzing MTN deficiency, it has provided a nonpathogenic model system for these studies. A metabolite study of another nonpathogenic *pfs* knock-out strain *E. coli* (MG1655) showed that it displayed up to 50% increases in SAM and SAH concentrations.⁴² While these data are interesting, neither of these strains allow the analysis of the effect of *pfs* gene deletion on virulence. However, these strains provide tools for proteomic analysis of adaptations to MTN deficiency, such as additional enzyme production or expression of enzymes used in potential alternate metabolic pathways.

As mentioned previously, SAM is involved in radical reactions that produce vitamins that are required for enzymes to function properly. Inhibition of MTN would be expected to cause accumulation of inhibitory levels of 5'dADO that in turn act to suppress the enzymes responsible for production of these vitamins. This is a possible cause for the growth delays reported in various inhibition studies.^{40,41} Reduced vitamin production can be analyzed by comparing the activity of enzymes found in central carbon metabolism that require lipoate, thiamine, or biotin cofactors, such as the pyruvate dehydrogenase and α -ketoglutarate dehydrogenase complexes, in the MTN KO strain to the WT strain. The MTN KO strain could show differences in the activity of alternate metabolic pathways, such as lactate dehydrogenase or alcohol dehydrogenase, that are adapted due to MTN deficiency (Figure 16).

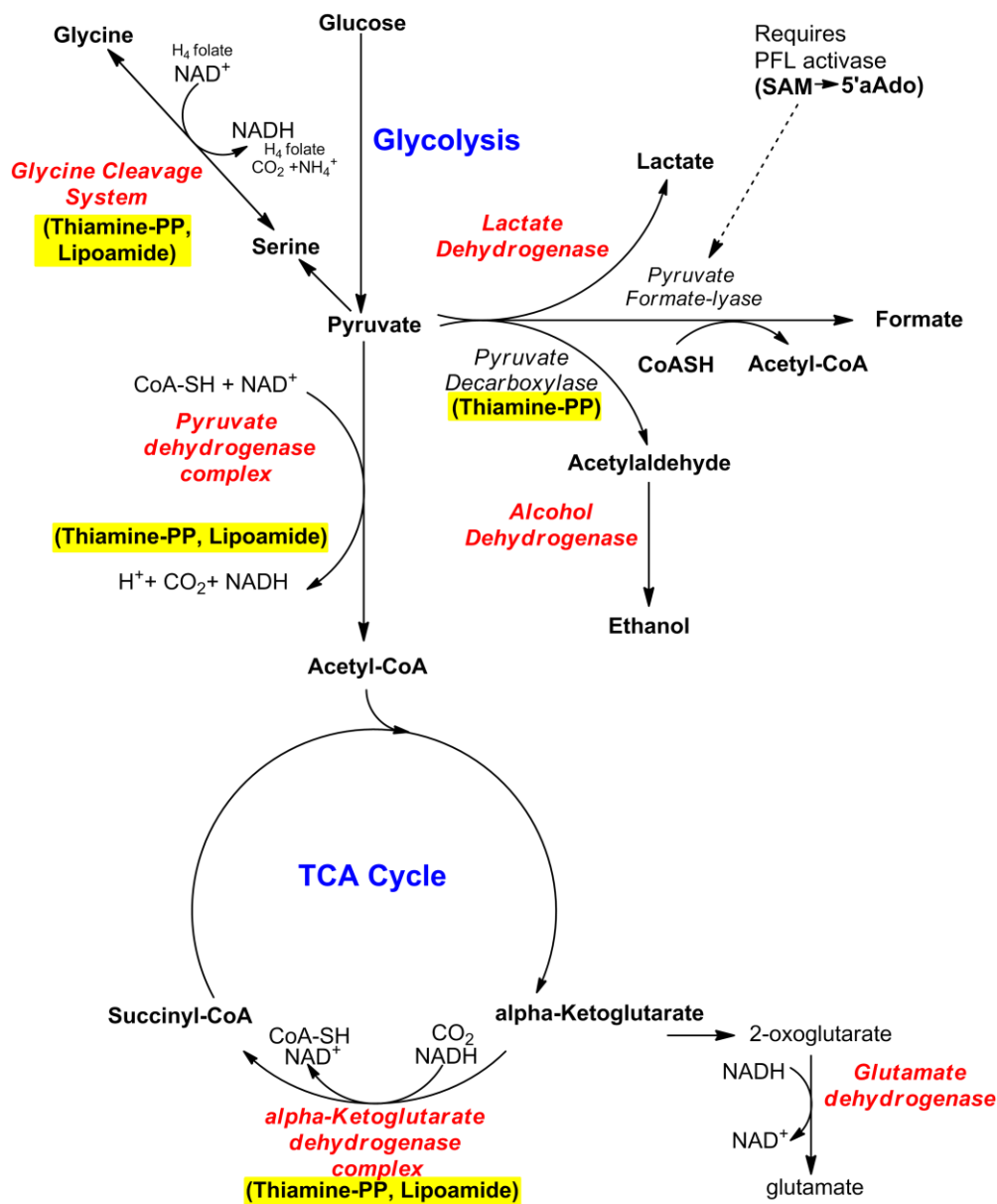


Figure 16. Central carbon metabolism with highlighted aspects affected by MTN deficiency. The specific enzymes or enzyme complexes of interest in this study are noted in red. Essential enzyme cofactors directly related to SAM radical reactions are highlighted in yellow.

Summary

MTN is a critical enzyme required for bacterial metabolism and is a potential target of novel antibiotics. Inhibition of MTN causes accumulation of potent feedback inhibitory nucleosides that have significant effects on SAM metabolic pathways. The effects range from the disruption of quorum sensing to the lack of methionine salvage. While MTN inhibitors have shown limited bactericidal activity, they could be combined with other treatments to enhance antibiotic responses or improve host immune system removal of the bacterial infection.

To fully understand the complete effects of MTN inhibition, genetic knockouts (MTN KO) of the *pfs* gene have been created in prior work.^{42,43} Removing the *pfs* gene allows for the maximal level of MTN inhibition and provides a standard to validate MTN as a drug target, and to use as a comparative tool to predict the effects of drug inhibition. All of the MTN KO strains have shown growth deficiencies, probably due to the inhibitory feedback effects of the nucleosides MTA, SAH, and 5'dADO.^{5,42,43} Since MTN activity is responsible for directly producing the S-ribosylhomocysteine precursor for *luxS* dependent AI-2 synthesis, it is also probable that MTN deficiency will affect quorum sensing dependent events proposed to be involved in biofilm formation and virulence.

In the following chapters, the potential of MTN inhibition as a target for antibiotic development have been investigated using a strain of pathogenic *E. coli* O157:H7. To understand how complete drug inhibition of MTN would affect this pathogen, a genetic knock-out of the *pfs* gene was created (MTN KO strain). The WT and MTN KO strains were subject to a variety of analyses to establish the effects on growth, biofilm formation,

and virulence. Supplementation studies (with vitamins and autoinducer-2) were designed to explore the potential mechanisms of antibiotic action. Further investigations of metabolic enzyme activity in central carbon metabolism involved the use of a non-pathogenic *E. coli* RK4353 MTN KO strain compared with its isogenic parental WT strain. For these studies, a directed investigation was performed on various enzymes that were predicted by proteomic data to be affected by MTN deficiency due to their dependence on vitamins for activity. Overall, the MTN KO strain showed defects in growth and virulence that appeared to be at least partially due to vitamin dependence.

CHAPTER TWO: MATERIALS AND METHODS

Creation of Electrocompetent Cells

E. coli O157:H7 strain (ATCC 43894) was streaked for isolation on LB plates and grown overnight at 37 °C. An isolated colony was used to inoculate 200 mL fresh LB media. Cells were grown at 37 °C at 225 RPM until the culture optical density at 600 nm (OD₆₀₀) reached ~ 0.5. Cells were subsequently heat shocked for 10 minutes at 42 °C with shaking, followed by 15 minutes on ice with rotation. Cells were harvested by centrifuged at 8,000 xg for 15 minutes at 4 °C, and resuspended in 8 mL of ice cold 20% glycerol. The culture was split into eight 2 mL centrifuge tubes and centrifuged at 10,000 xg for 1 minute. The supernatant was removed by aspiration, and the cell pellet washed three times with ice cold 20% glycerol. Competent cell pellets were resuspended in 50 µl ice cold 20% glycerol and stored at -80°C.

Generation of MTN Knockout (MTN KO) Strain Using the λ-Red System

Deletion of the *pfs* gene was accomplished using the λ-red system.⁹⁰ Briefly, the recombinase encoding plasmid pKD46 was introduced into competent cells using electroporation (2000 V, 200 Ω, and 25 µF). Following electroporation, samples were recovered in SOC media and incubated at 37 °C with horizontal shaking for 1.5 hours. Transformants were selected on LB plates supplemented with ampicillin (100 µg/mL) and chloramphenicol (25 µg/mL) plates and grown overnight at 37 °C. An isolated colony was selected and inoculated into 200 mL of fresh LB ampicillin (100 µg/mL)

broth and grown at 37 °C until an OD₆₀₀ of 0.1 was reached. Recombinase activity was induced by the addition of arabinose to 10 mM, and continued incubation at 37 °C until the culture reached an OD₆₀₀ of 0.4. pKD46⁺ cells were made electrocompetent as described above.

To create the MTN KO strain, the chloramphenicol resistance (Cm^r) cassette in pKD3 was amplified by polymerase chain reaction (PCR) using primers containing flanking *pfs* homologous sequences: *pfs*LF-*TTAGC CATGT GCCAG TTTCT GCACT AGTGA CTCAA CCATC AGTGT AGGCT GGAGC TGCTT CG-3'*; *pfs*LR-*ATGAA AATCG GCATC ATTGG TGCAA TGGAA GAAGA AGTTA CGCTC ATATG AATAT CCTCC TTA-3'* (*pfs* sequences are italicized). The PCR reaction contained 20 ng pKD3 template, 50 pmol primer (each) and 1 unit One *Taq* Hot Start DNA polymerase (New England BioLabs, Ipswich, MA). Cycling conditions consisted of 95 °C (7 min), followed by 35 cycles of 94 °C (15 sec), 50 °C (30 sec), and 72 °C (90 sec). The 1.1 Kb PCR product was purified using a Perfectprep® Gel Cleanup kit (Eppendorf, Hauppauge, NY) and quantified by UV spectrophotometry. The purified chloramphenicol cassette (100 ng) was introduced into competent *E. coli* O157:H7 cells containing pKD46 using the conditions described above. Successful transformants were selected on LB agar plates containing chloramphenicol (25 µg/mL). The transformants (Δpfs , amp^r, cm^r) were cured (25 µg/mL), but lacking ampicillin. Loss of MTN activity in the *E. coli* O157:H7 strain (Δpfs , amp^s, cm^r) was confirmed by enzyme assay and western blot analysis (see later section).

Generation of MTN Knock-In (MTN KI) Strain

A MTN KI strain was created from the *E. coli* O157:H7 MTN KO strain in order to study the effect of gene reconstitution on the cellular phenotype. The *E. coli* O157:H7 (Δpfs , cm^f) was made electrocompetent as described above. The plasmid pMTN²⁹ was introduced using the electroporation conditions described for pKD46 (above), and positive transformants selected by growth on LB containing ampicillin (100 $\mu\text{g}/\text{mL}$) and chloramphenicol (25 $\mu\text{g}/\text{mL}$).

Analysis of MTN Activity: Preparation of Bacterial Lysates

Fresh 5 mL cultures of *E. coli* O157:H7 WT, MTN KO, and MTN KI strains were prepared in LB broth containing appropriate antibiotics and grown overnight at 37 °C with shaking. Cultures were diluted into 100 mLs of fresh LB broth and re-incubated for 24 hours at 37 °C with shaking. Bacterial cells were harvested by centrifugation (5000 $\times g$ / 15 min) and resuspended in 1 mL PBS. Cells were lysed by sonication on ice using a Misonix Sonicator 300 (power setting 7, 30 sec pulse, 1 min cooling, 2.5 min total sonication). The lysates were centrifuged at 5,000 $\times g$ for 15 min at 4 °C to remove debris, and the cell lysates transferred to fresh tubes. The protein concentration of the lysates was determined using BioRad reagent (BioRad, Hercules, CA). Lysates were stored at -80 °C until analyzed for MTN by immunoblot and enzyme assay.

Analysis of MTN Activity: Immunoblot Assay

The presence of MTN protein in the WT, MTN KO, and MTN KI strains was analyzed by SDS-PAGE and western blot. Samples of cell lysate proteins (20 $\mu\text{g}/\text{lane}$) were electrophoresed (66 mA/45 min) on 15% acrylamide gels using a BioRad Miniprotean system. An EZ-Run Prestained Rec Protein ladder (Thermo Fisher

Scientific) was used as a standard to assess molecular weight. Separated proteins were transferred to nitrocellulose by electroblotting at 10V for 18 hours. The blot was blocked using 10x Superblock (Thermo Fisher Scientific) on a Millipore SNAP i.d. system. The presence of MTN in the lysates was detected using a murine monoclonal anti-MTN antibody²⁶ (1:1000 dilution) and goat-anti-mouse Ig-HRP conjugate antibody (Thermo Fisher Scientific). Blots were developed using Pierce ECL Western Blotting substrate and Kodak X-Omat x-ray film.

Analysis of MTN Activity: Enzyme Assay

Activity of MTN in lysates of *E. coli* O157:H7 WT, MTN KO, and MTN KI strains was determined by monitoring loss of absorbance at 275 nm accompanying the cleavage of MTA into MTR and adenine using the extinction coefficient $1.6 \text{ mM}^{-1} \text{ cm}^{-1}$.³¹ The enzyme reactions contained 50 mM potassium phosphate (pH 7) and 100 μM MTA in a final volume of 990 μL , and were initiated by the addition of 10 μL (40 μg) of lysate. The absorbance at 275 nm was measured using a Varian Cary 50 spectrophotometer. Specific activities were calculated in U/mg (1U = 1 $\mu\text{mol}/\text{min}$ MTA degradation).

Cell Growth Assays

To determine the effect of MTN status on growth, fresh overnight cultures of *E. coli* O157:H7 WT, MTN KO, and MTN KI strains were prepared in 5 mL Davis Minimal Media (per liter: 7 g KH_2PO_4 , 2 g K_2HPO_4 , 1 g $(\text{NH}_4)_2\text{SO}_4$, 0.5 g Na citrate $2\text{H}_2\text{O}$, 0.025 g MgSO_4) supplemented with 0.2% glucose (DMMG). The overnight cultures were diluted 1:10,000 and 200 μL used to inoculate triplicate wells in a 96-well plate. The plate was incubated in a Synergy HT plate reader (BioTek, Winooski, VT) at 37 °C with shaking, and absorbance readings at 600 nm were taken every 15 minutes for 72 hours.

The assay was repeated with WT and KO strains with the DMMG medium supplemented with either lipoate, thiamine, biotin, dihydroxypentane dione (DPD), or a mix of all four supplements (1-100 μ M).

Biofilm Assays

Cultures of the *E. coli* O157:H7 WT, MTN KO, and MTN KI strains were established in the 96-well plates as described for the cell growth assays above. Cultures were grown for 48 hours at 30 °C, which was optimal for biofilm formation. The media was then removed and the wells washed three times with PBS (250 μ L) to remove loosely bound cells. Biofilms were fixed using 250 μ L of a 1% paraformaldehyde solution in PBS for 1 hour at 4 °C. Subsequently, wells were washed three times with water, and the adhered biofilms stained with 250 μ L 0.1% crystal violet in PBS for 15 min.⁹³ Plates were washed three to five times with water, and the bound crystal violet solubilized in 250 μ L of an ethanol:acetone (80:20) solution for 15 min. Solubilized material (200 μ L) was transferred to a fresh 96-well plate and an absorbance reading at 590 nm measured using a BioTek Synergy HT plate reader. The assay was repeated with WT and KO strains grown in DMMG supplemented with DPD, a vitamin mix (1 μ M each biotin, lipoate, thiamine), or DPD and a vitamin mix.

A second assay was performed to more readily visualize biofilm production. Overnight cultures of the three strains were prepared as described above and diluted (1:10,000) into 3 mL of fresh DMMG in a 5mL polystyrene culture tube. Cultures were incubated for 48 hr at 30 °C. Biofilms were stained as describe above, with the modification that the volumes for all washing, fixing, and staining steps were adjusted to 3.2 mL. Stained biofilms were photographed using a digital camera. The assay was

repeated with WT and KO strains grown in DMMG media supplemented with either DPD, vitamin mix, or DPD and vitamin mix as previously described.

The qualitative appearance of biofilms formed by the three strains was also examined by confocal microscopy. Biofilms were grown on plastic coverslips partially submerged in 5 mL cultures in DMMG media. Biofilms on coverslips were washed and fixed as described above, but the volumes of solutions were adjusted to 5.5 mL for each step. After the final wash, the coverslips were stained with 1 mL 0.1% (w/v) acridine orange in PBS for 1 hour in the dark. Coverslips were rinsed lightly with PBS and the biofilms visualized at 600x magnification using a Zeiss LSM Meta 510 confocal microscope set to an excitation wavelength of 476 nm. Standard and Z-stack (20 slices) images were analyzed using Zen 2012 digital imaging software (Carl Zeiss Microscopy, Oberkochen, Germany).

Adherence Assays

The adherence of *E. coli* O157:H7 WT, MTN KO, and MTN KI strains to mammalian epithelial cells was studied using a previously established protocol.⁹⁴ Briefly, bovine Mac-T epithelial cells were cultured in DMEM supplemented with 5% FBS, penicillin (100 U/mg), and streptomycin (100 µg/mL) at 37 °C with 5% CO₂. When cells were approximately 70% confluent, they were harvested and seeded in triplicate (~1 x 10⁵ cells) onto coverslips in a 6-well plate. When cells on the coverslips were approximately 70% confluent, the coverslips were washed with antibiotic-free DMEM with 5% FBS. For adherence assays, *E. coli* O157:H7 WT, MTN KO, or MTN KI cultures were grown overnight in LB broth at 37 °C with shaking, and diluted (1:10,000) into DMEM. Cells were stained by addition of Syto-9 (10 µg/mL) for 15 min, followed

by three washes with DMEM. Infections were initiated by addition of 1 mL bacterial cells ($\sim 1 \times 10^6$ cells) to the surface of the mammalian cells. Co-incubation of bacterial and mammalian cells occurred for 3 hours at 37 °C with 5% CO₂. The wells were then washed with PBS and the cover slips fixed with 4% paraformaldehyde in PBS for 10 min at room temperature. Coverslips were washed twice with PBS, permeabilized with 0.1% Triton X-100 in PBS for 5 min, and non-specific binding sites blocked with 1% BSA in PBS for 20 min. Cellular actin was stained with TRITC conjugated phalloidin dye (5 µg/mL in PBS) for 40 min. Coverslips were washed twice with PBS, dried, treated with ProLong Gold antifade reagent (Invitrogen, Carlsbad, CA) and mounted on glass slides with clear nail polish. Adherent bacterial cells were visualized at 1000x magnification using a LSM Meta 510 confocal microscope with excitation wavelengths set to 348 nm (DAPI), 476 nm (Syto-9), and 557 nm (TRITC). Images were analyzed using Zen 2012 digital imaging software (Carl Zeiss Microscopy, Oberkochen, Germany).

To quantify bacterial adherence, bovine Mac-T cells were prepared as described above in a 6-well plate. Cultures were grown until they reached approximately 70% confluence, and then infected with WT, MTN KO, or MTN KI strain cells grown overnight in DMMG, DMMG supplemented with DPD (25 µM), DMMG with vitamin mix (100 µM each lipoate, biotin, and thiamine), or DMMG with DPD (25 µM) and vitamin mix (100 µM each). Co-incubation continued for 3 hours at 37 °C in 5% CO₂ atmosphere. Subsequently, bacterial cultures were aspirated, the wells washed three times with PBS, and the mammalian cells lysed by treatment with 0.1% Triton X-100 in PBS for 15 min. Dilutions of detergent lysates were plated onto LB agar, incubated overnight

at 37 °C, and the adhered cells enumerated by colony counting. Colony forming units (CFU) were expressed as a percentage relative to the adhered WT CFU (set at 100%).

Vero Cell Cytotoxicity Assay

Shiga toxin production was measured using a Vero cell cytotoxicity assay, essentially as described.⁸⁵ To compare *E. coli* O157:H7 WT and MTN KO strain Shiga toxin production, cells were cultured overnight at 37 °C with shaking in 2 mL DMMG containing either: 1) no supplement; 2) 25 µM DPD; 3) vitamin mix (100 µM each lipoate, biotin and thiamine); or 4) a mixture of DPD and vitamin mix. To prepare secreted Shiga toxin samples, cultures were centrifuged at 15,000 xg for 5 minutes, and the supernatants filter sterilized and stored at -20 °C. The periplasmic Shiga toxin samples were prepared by resuspending the cell pellets in 250 µL of polymyxin B (10 mg/mL) in PBS.⁹⁵ After shaking for 15 min at 37 °C, the samples were recentrifuged at 15,000 xg for 10 min, and the supernatant (containing the periplasmic proteins) was removed, filter sterilized, and stored at -20 °C until assayed.

Vero cells were cultured in DMEM supplemented with 5% FBS, penicillin (100 U/mg) and streptomycin (100 µg/mL) at 37 °C in 5% CO₂ atmosphere. For cytotoxicity assays, Vero cells were seeded into 96-well plates at a cell density of 1 x 10⁵ cells per well 24 hr prior to exposure to toxin. The media in each well was then replaced with 160 µL antibiotic-free DMEM and 40 µL of supernatant or periplasmic extract. All samples were tested in replicates of five. A positive control consisted of Vero cells exposed to 40 µL of ethanol. Negative controls (for cytotoxicity) consisted of untreated Vero cells, Vero cells treated with 40 µL of sterile DMMG, or Vero cells exposed to 40 µL of polymyxin B (10 mg/mL) in PBS. The plate was incubated for 48 hr at 37 °C in 5% CO₂

atmosphere. The media was then removed, and cells stained for 30 min with 100 μ L of 0.4% crystal violet in methanol. Excess dye was removed by rinsing the plate three times with distilled water. Bound dye was solubilized in ethanol:acetone (80:20) solution for 15 min and the absorbance at 590 nm quantified using a BioTek Synergy HT plate reader.

The percent cytotoxicity was calculated using the equation:

$$\% \text{ Cytotoxicity} = \left(\frac{OD_s}{OD_t} \right) \times 100$$

where OD_s is the difference in optical density at 590 nm between the sample and the negative controls, and OD_t is the difference in optical density at 620 nm between the ethanol positive control and negative controls.

Type III Secretion System Protein Assay

The ability of WT, MTN KO, and MTN KI strains to secrete the type III secretion system proteins EspB and Tir was measured by the enzyme-linked immunoabsorbent assay (ELISA).⁶⁴ Briefly, bacterial cultures were grown overnight in 10 mL M-9 minimal medium supplemented with 44 mM NaHCO_2 , 8 mM MgSO_4 , 0.4% glucose, and 0.1% casamino acids at 37 °C in 5% CO_2 atmosphere.⁶⁴ Cell culture supernatants were collected by centrifugation (10,000 x g/10 min) and concentrated 100-fold by ultrafiltration (Amicon Ultra 3K) according to the manufacturers specification. Samples were stored at -20 °C until assayed.

ELISA plates were coated with 100 μ L concentrated cell culture supernatant in binding buffer (20 mM Tris, pH 7.4, 150 mM NaCl, 1 mM CaCl_2 , 1 mM MgCl_2 , 1 mM MnCl_2 .) overnight at 4 °C. Wells were washed twice with PBS and blocked with 0.5% BSA in PBS for 1 hr at 37°C. EspB or Tir proteins were detected using monoclonal anti-EspB or anti-Tir antibodies (kind gift of Dr. Brett Finlay at the University of British

Columbia) diluted 1:1000 in PBS + 0.05% Tween 20. After 1 hr in primary antibody, the ELISA plates were washed three times with PBS and incubated for an additional 1 hr with a horseradish peroxidase-conjugated goat anti-mouse IgG secondary antibody (Thermo Fisher Scientific) diluted 1:1000 in PBS + 0.05% BSA. Plates were washed three times with PBS and developed using horseradish peroxidase substrate (0.2 mg o-phenylene diamine in an 50 mL 80 mM citrate–phosphate buffer, pH 5.0). Absorbance readings (490 nm) were collected for 30 min using a Biotek Synergy HT plate reader.

Hemolysin Assays

The amount of hemolysin produced by the WT, MTN KO and MTN KI strains was determined using a sheep red blood cell (SRBC) lysis assay.⁹¹ Briefly, bacterial cultures and cell culture supernatants were prepared as described above for secreted Shiga toxin. Serial dilutions of the cell culture supernatants were prepared in PBS and 100 μ L added to triplicate wells in a 96-well plate containing an equal volume of 3% SRBCs in PBS. The positive and negative controls consisted of SRBC lysis buffer (150 mM NH₄Cl, 10 mM KHCO₃, 0.1 mM EDTA), and PBS, respectively. Plates were incubated at 37°C with shaking for 30 min. Absorbance readings at 620 nm were collected in a BioTek Synergy HT plate reader. Hemolysin activity was calculated using the following equation:

$$\% \text{ Hemolysis} = \left(\frac{1 - OD_s}{OD_t} \right) \times 100$$

where OD_s is the difference in optical density at 620 nm between the sample and the SRBC lysis buffer positive control, and OD_t is the difference in optical density at 620 nm between the PBS negative control and RBC lysis buffer positive control.

Metabolic Enzyme Analysis

To analyze the effect of MTN deficiency on enzyme activities in central carbon metabolism, fresh 5 mL overnight cultures of the nonpathogenic *E. coli* RK4353 WT, MTN KO, and MTN KI strains were grown in DMMG at 37 °C with shaking. Overnight cultures were diluted into 500 mL of fresh DMMG for a total of six cultures per strain and incubated at 37 °C with shaking. The cultures were monitored spectrophotometrically until the absorbance at 600 nm reached 0.5 (mid-log phase). At this point, three 500 mL cultures from each strain were centrifuged at 5000 xg for 10 min to pellet the cells. The supernatant was removed and the cell pellet was stored at -80 °C. The remaining three cultures of each strain were cultured for 4 hours after reaching an absorbance (600 nm) of ~1.0 (stationary phase) and the cell pellets recovered by centrifugation at 5000 xg for 10 min. Cell pellets were extracted by vortexing in 5 mLs of B-PER bacterial protein extraction reagent (Pierce) for 15 minutes, and insoluble debris removed by centrifugation at 15,000 x g for 15 min. Lysate supernatants were removed and the protein concentration determined using a BioRad assay as described by the manufacturer Pyruvate dehydrogenase (PDH), lactate dehydrogenase (LDH), alcohol dehydrogenase (ADH), glutamate dehydrogenase (GDH), and α ketoglutarate dehydrogenase (KDH) activities in mid-log and stationary phase enzyme samples from the RK4353 WT, KO, and KI strains were measured using a colorimetric coupled assay and following the absorbance change at 570 nm.⁹⁶ Enzyme reactions were assembled in a 96-well plate, with each well containing 20 μ L of a detection reagent (1 mM MTT, 150 mM NAD⁺, 50 μ M PES) and 170 μ L of a substrate buffer (500 mM KPhos, pH 8.0, 10

mM MgCl₂, 3 mM DTT) that contained either 50mM pyruvate, 1mM CoA (for PDHC); 50 mM lactic acid (for LDH); 50 mM ethanol (for ADH); 50 mM glutamate (for GDH); or 50 mM α -ketoglutarate, 1 mM CoA (for KDH). Enzyme reactions were initiated by the addition of 10 μ L of lysate. The increase in absorbance at 570 nm was measured every 30 sec for 30 min using a BioTek Synergy HT plate reader. Average specific activities were calculated using the Beer-Lambert law ($A=\epsilon lc$) using an extinction coefficient of 13 mM⁻¹ cm⁻¹. All reactions were run at least three times. The results were expressed in U/mg, where 1 U = 1 μ mol NADH created per min of mg of lysate protein.

CHAPTER FOUR: RESULTS AND DISCUSSION

Creation and Analysis of a Genetic MTN Knock-out in *E. coli* O157:H7

Creation of the MTN gene knock-out strain of *E. coli* O157:H7 was achieved using the λ -red recombination system. The coding region for *pfs* (MTN) was replaced with a chloramphenicol resistance cassette (Figure 17). Successful transformation was difficult to obtain. Multiple attempts (> 10) to create the MTN KO failed. Probably this was due to the severe effect on growth caused by the MTN deletion. Eventually, an experiment resulted in two very small colonies surviving selection on chloramphenicol plates. Both colonies were repeatedly propagated under chloramphenicol selection to ensure gene deletion. Gene deletion was further confirmed by PCR (data not shown). The creation of a MTN knock-in strain was achieved by transforming the pMTN plasmid into MTN KO cells and selecting for ampicillin resistance. The resulting KI strain was MTN⁺ Cm^r Amp^r, and expressed MTN under the control of an IPTG inducible promoter.

To ensure that the MTN KO strain had completely lost the ability to produce MTN, western blot and nucleosidase assays were performed (Figure 17). A monoclonal α -MTN antibody readily detected the 24.5 KD nucleosidase in western blots of cell lysates of the WT and MTN KI strains, but not in lysates of the MTN KO strain (Figure 17 B). Similarly, MTA nucleosidase activity was detected in lysates of the WT and MTN KI strains. The MTN KO strain showed significant loss of nucleosidase activity relative to the WT strain ($p < 0.05$). The residual enzyme activity in the MTN KO strain was at the limit of detection in the assay (Figure 17 C). While theoretically no MTN activity should

be present in the MTN KO strain, the small amount of substrate conversion in the assay could be due to solvent hydrolysis or the activity of nonspecific nucleosidases present in the lysate (e.g., AMP nucleosidase or purine nucleoside phosphorylase).

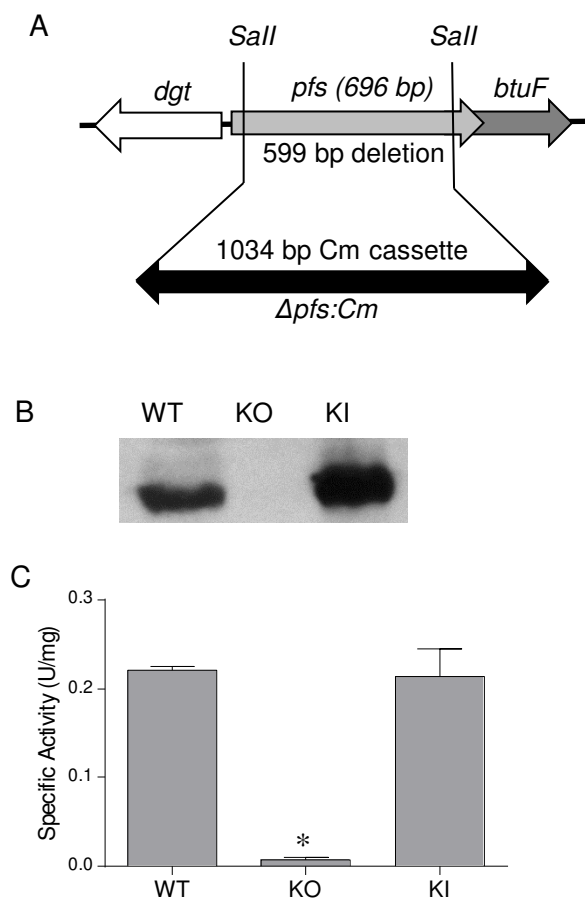


Figure 17. Analysis of the *E. coli* O157:H7 MTN knock-out strain. (A) Representation of the *dgt-pfs-butF-yadS* region of the *E. coli* O157:H7 chromosome map. The $\Delta pfs:Cm$ knockout strain was created by a 599 bp in-frame deletion of the *pfs* gene and insertion of the 1034 bp Cm^r cassette. (B) Western blot analysis of MTN in WT, MTN KO, and MTN KI strains. MTN in cell lysates (20 μ g protein/lane) was detected using a monoclonal mouse α -MTN antibody followed by staining with a goat α -mouse Ig-HRP conjugate. (C) Specific activities of cell lysates (40 μ g protein /assay) were analyzed by UV enzyme assay (275 nm) using 100 μ M MTA substrate. (1 U = 1 μ mol/minute, n = 3, \pm SEM) * denotes $p < 0.05$ by 1way ANOVA.

Effect of MTN Deficiency on Growth

MTN deficiency severely decreased growth rates in the MTN KO strain. This was initially evident in the small colony size of the MTN KO strain, and intermittent difficulty in growing overnight stock cultures in minimal media. In 96-well plate growth assays, an 18 hour delay in achieving mid-logarithmic phase growth was typically observed for the KO strain when compared to the WT (Figure 18 A). However, the MTN KO strain did eventually reach the same cell density as the WT culture. The MTN KI strain growth closely matched the WT strain. This indicates that the growth delay in the MTN KO strain can be attributed to the loss of MTN activity.

Similar growth defects have been observed in other MTN KO strains constructed in the nonpathogenic *E. coli* RK4353⁶⁸ and *Neisseria meningitidis*.⁴³ In the initial report on the *E. coli* RK4353 MTN KO strain, investigators found a very strong reduction in growth in minimal media supplemented with methionine, and no growth in the absence of supplementation. These authors also reported that growth was restored in the MTN KO strain when it was transformed with a plasmid containing MTN.⁶⁸ This finding is similar to the results we show in Figure 18 A (KI black dashed line). The *Neisseria meningitidis* MTN KO strain also showed similar growth deficiencies, even in nutrient rich medium. Growth was restored in the *Neisseria* MTN KO strain when the MTN gene was reintroduced on a plasmid.⁴³

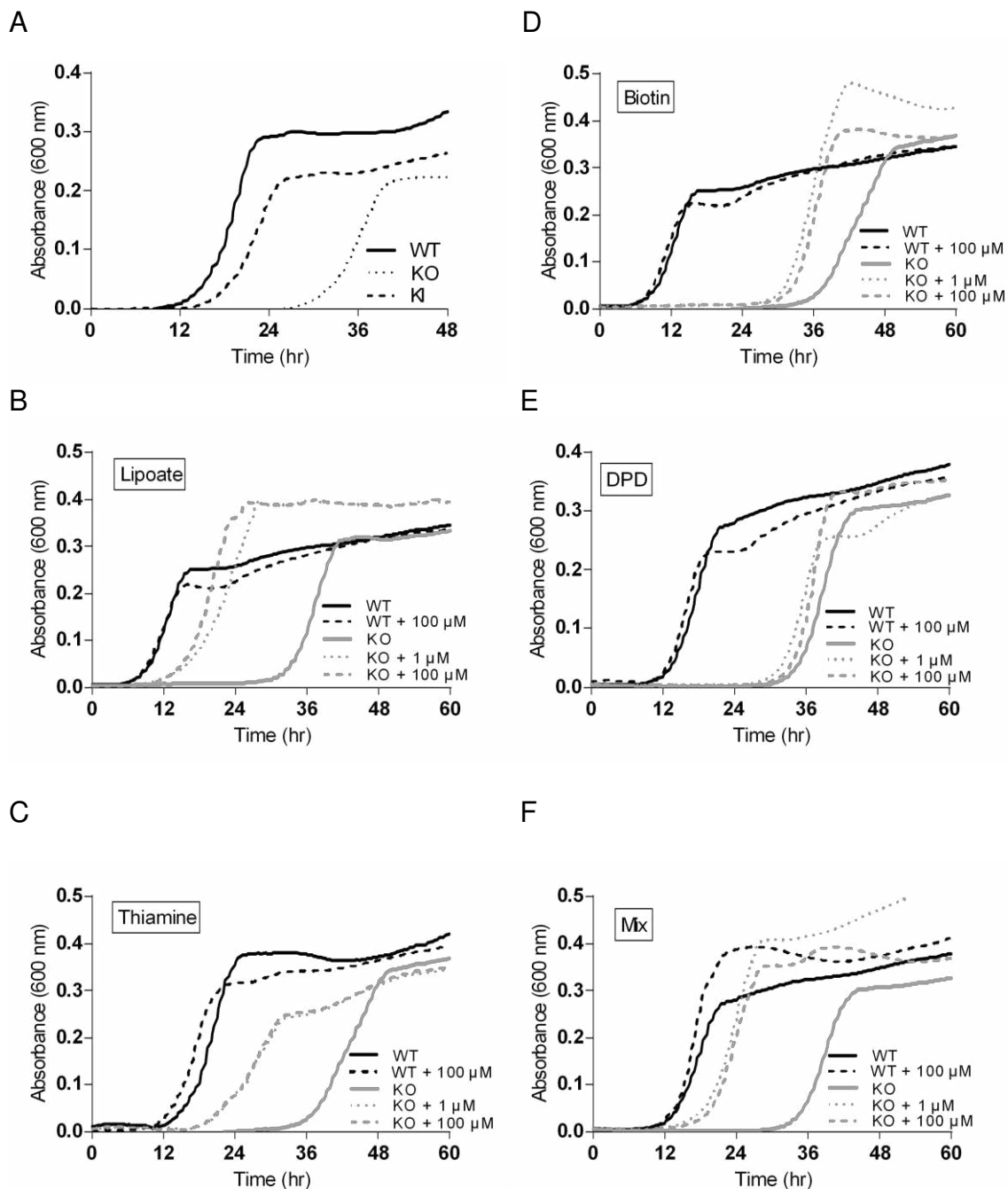


Figure 18. Comparison of growth of *E. coli* O157:H7 WT, MTN KO and MTN KI in Davis minimal media (A). Media was also supplemented with lipoate (B), thiamine, (C), biotin (D), DPD (E) and a mix of all the previous (F). Data shown is the average of three experiments with $n = 3$ replicates.

How loss of MTN activity caused growth delay in *E. coli* O157:H7 was probed by the addition of various vitamin supplements to the culture medium. Since MTN deficiency could result in an increase in 5'dADO concentration that would subsequently cause feedback inhibition of radical SAM reactions involved in vitamin synthesis^{10,82}, the effect of lipoate, thiamine and biotin supplementation on cell growth was explored (Figure 18 B, C, D). Of the three vitamins, lipoate supplementation showed the greatest effect on MTN KO strain growth. When MTN KO strain cultures were supplemented with 1 μ M or 100 μ M lipoate (Figure 18 B, gray dashed lines), the growth rate was dramatically improved and the time to achieve mid-log phase growth was shifted to within roughly 6 hours of the WT culture. Thiamine supplementation (1 μ M or 100 μ M) showed a less extreme effect on MTN KO strain growth with mid-log phase achieved at approximately 25 hours, or within 12 hours of WT growth (Figure 18 C, gray dashed lines). Lastly, biotin supplementation (1 μ M or 100 μ M) had the least effect on vitamin stimulated growth recovery in the MTN KO strain. Biotin supplemented cultures reached mid-log phase only 8 hours sooner than the unsupplemented MTN KO culture (Figure 18 D, gray dashed lines).

MTN gene deletion disrupts the primary pathway to AI-2 production by preventing hydrolysis of SAH to S-ribosylhomocysteine (SRH) that would block subsequent *luxS* mediated synthesis of DPD. While a second potential path to DPD synthesis has been reported, it was not found to be a significant source of AI-2 in *E. coli*.⁸¹ In addition, prior work in *Neisseria* and a nonpathogenic *E. coli* strain (RK4353) showed that MTN gene deletion abolished AI-2 production.^{43,71} To examine the potential role of AI-2 on *E. coli* O157:H7 growth, cultures of WT and MTN KO strains were

supplemented with DPD, the precursor to AI-2. DPD did not appear to improve growth rates in either the WT or MTN KO strain (Figure 18 E). These results are similar to those reported for *N. meningitidis*,⁴³ and support the assertion that the observed growth defects are not autoinducer-2 dependent.

In summary, the defects in planktonic cell growth due to MTN deficiency could largely be attributed to inhibition of radical SAM reactions that resulted in decreased LipA, BioB, and ThiH synthesis of lipoate, biotin and thiamine, respectively.¹⁰ However, culture supplementation with a mixture of all three vitamins and DPD failed to completely restore growth, suggesting that other deficiencies were also present in the MTN KO strain (Figure 18 F). Overall, the results of these growth studies suggest that MTN inhibitors could exert their antibiotic effect due to interruption of radical SAM reactions because of feedback inhibition by 5'dADO. In addition, the observation that the MTN KO strain did eventually reach a culture density similar to the WT strain suggests that MTN inhibitors will behave in a bacteriostatic rather than bactericidal manner.

Effects of MTN Deficiency on Biofilms

When biofilm production was examined in a polystyrene-tube growth assay, obvious culture differences were observed by crystal violet staining (Figure 19 A). The WT strain showed heavy biofilm growth, particularly at the liquid-air interface. The MTN KO strain showed little crystal violet staining. Culture supplementation with DPD failed to restore biofilm growth. Similar to the planktonic growth studies, vitamin supplementation (100 μ M lipoate, thiamine, biotin) restored MTN KO biofilms to approximately WT levels. The reduction in biofilm due to MTN KO was further quantified in a 96-well plate assay. Wells containing 48 hour cultures of WT and MTN

KO cells (+/- supplementation) were stained with crystal violet and the biofilms quantified by measuring the spectrophotometric absorbance at 595 nm. The results showed that biofilms were reduced by greater than 80% in the MTN KO strain when compared to the WT strain (Figure 19 B). Again, vitamin supplementation restored MTN KO biofilms, whereas the addition of DPD did not.

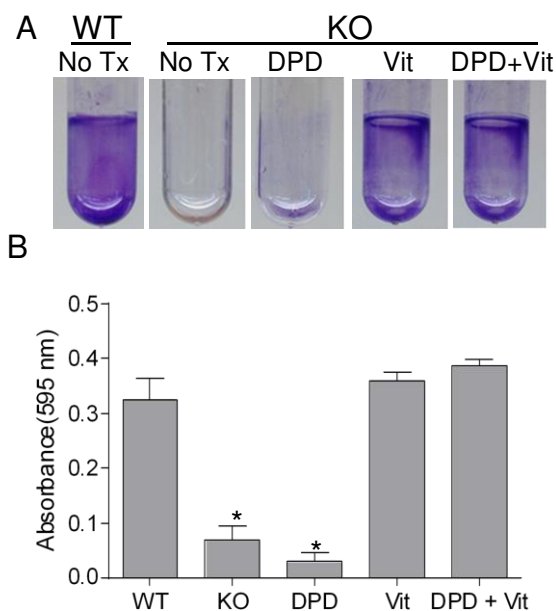


Figure 19. Comparison of biofilm production by *E. coli* O157:H7 WT and MTN KO strains. (A) Crystal violet staining in 48 hour biofilms grown in minimal media. MTN KO cultures were supplemented with 25 μ M DPD, 100 μ M vitamin mix (Vit), or DPD and vitamin mix (DPD + Vit). (B) Quantitative data of crystal violet stained biofilms (\pm SEM, n = 3). * denotes $p < 0.05$ by One-way ANOVA

The effect of MTN KO on *E. coli* O157:H7 biofilm formation was also examined by confocal microscopy (Figure 20). In these studies, biofilms were grown directly on plastic cover slips and visualized by staining with acridine orange. As the figure shows, the WT and MTN KI strains formed heavy biofilms (Figure 20 A). By comparison, the MTN KO strain formed only a weak disperse biofilm. Three dimensional pictures created from serial images through the depth of the biofilm further show the mature architecture

of the WT and MTN KI strain biofilms (Figure 20 B). Biofilm formation in the MTN KO was too weak to assemble a three dimensional image.

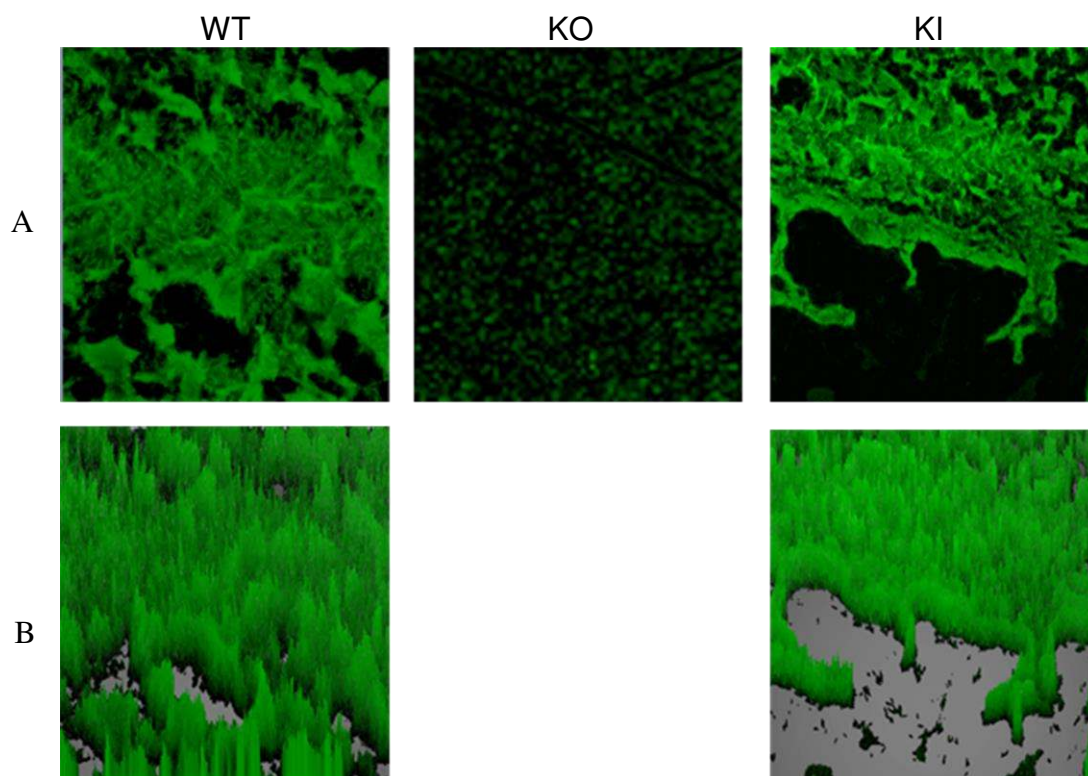


Figure 20. Confocal microscopy of biofilms produced by *E. coli* O157:H7 WT, MTN KO, and MTN KI strains. Biofilms were grown for 48 hours on plastic coverslips and stained with acridine orange. (A) Images taken at 630x magnification. (B) 3-D images created from Z-stacks at 630x magnification. Biofilms were insufficient in the MTN KO strain to create a 3-D image.

Previous work has demonstrated the disruption of *E. coli* O157:H7 biofilms using MTN inhibitors.⁷¹ However, biofilm formation was only reduced by 18% when compared to the untreated control. Potentially this modest effect on biofilms could be attributed to poor drug permeability into the *E. coli* cells. On the other hand, the same drug treatment caused a 70% reduction in *Vibrio cholera* biofilms.⁷¹ Overall, our studies indicate that biofilm formation in *E. coli* O157:H7 is dependent on the availability of vitamins used by metabolic enzymes, rather than AI-2 signaling. In this regard, the reports in the literature

of the effects of AI-2 on biofilm formation are not consistent. For the majority of these studies, *luxS* KO strains were examined since they are unable to make DPD, the precursor to AI-2.⁷²⁻⁷⁵ The loss of biofilm formation seen in the *luxS* KO strains was attributed to lack of AI-2 signaling, but nutrient supplementation was not investigated. In one study, supplementation of WT *E. coli* O157:H7 with DPD increased biofilm formation by 30-fold.⁷² In our studies, DPD treatment did not cause an increase in WT biofilms (not shown). However, the abundant biofilms formed by the WT strain we studied may have masked any overt influence by DPD, and we did not examine early stages of biofilm formation.

Effect of MTN Deficiency on Virulence Factors

Adherence

The effect of MTN deficiency on virulence was initially examined by comparing the ability of the WT and MTN KO strains to adhere to mammalian cells. Cows are the main reservoirs for *E. coli* O157:H7, thus the ability of the bacteria to adhere to cultured bovine epithelial cells was measured. Using confocal microscopy, the adherence of the WT strain to the surface of bovine Mac-T cells was readily apparent (Figure 21 A). To find adherent MTN KO cells was difficult, as these events were visible on fewer than 1 in 50 microscopic fields (Figure 21 B).

Microbial adherence was also measured by counting colony forming units (CFUs) after bacteria were incubated with bovine Mac-T cell cultures. In these experiments, bacterial cells were added to the mammalian cell culture at an MOI of ~100. Adhered bacterial cells were liberated following detergent lysis of the mammalian cell culture and enumerated by counting the colonies that appeared on LB agar plates. As the graph in

Figure 14 C shows, the MTN KO strain exhibited an 85% decrease in adherence to bovine Mac-T cells relative to the WT strain. Similar results were obtained when the experiment was performed with the human HeLa cell line (not shown). There are no other reports of adherence studies using MTN KO strains. However, the adherence and infectivity of *luxS* mutants has been studied.^{43,77} Epithelial cell adherence was reported to be reduced by two orders of magnitude in a *luxS* mutant strain of enteropathogenic *E. coli* (EPEC).⁷⁷ In the pathogen *N. meningitidis*, *luxS* mutants were attenuated for the ability to cause bacteremia in mice.⁴³ These studies established that loss of AI-2 synthesis decreased bacterial virulence. They suggest that interruption of MTN activity could similarly be expected to reduce virulence since AI-2 is also not made in the MTN KO strain.

Since nutrient supplementation caused profound effects on bacterial growth and biofilm production, the effect of similar supplementation was studied in the mammalian cell adherence assay. Overnight culture of the bacterial cells with either DPD (25 μ M), vitamin mix (100 μ M each lipoate, thiamine, biotin), or both (DPD + Vit) failed to improve adherence of the MTN KO strain to Mac-T cells (Figure 21 C). This data indicates that adherence is not due to AI-2 signaling or vitamin dependent metabolism. Other studies suggest that *E. coli* O157:H7 adherence is influenced by AI-3 rather than AI-2 signaling.⁶⁷ In general, the conflicting reports of the effect of AI-2 signaling on bacterial adherence and virulence underscores the complexity of these processes. The failure of culture supplementation with DPD and vitamins to reverse the loss of adherence to mammalian cells by the MTN KO strain suggests that other factors (e.g., specific methylations, polyamines, etc.) are required for this event.

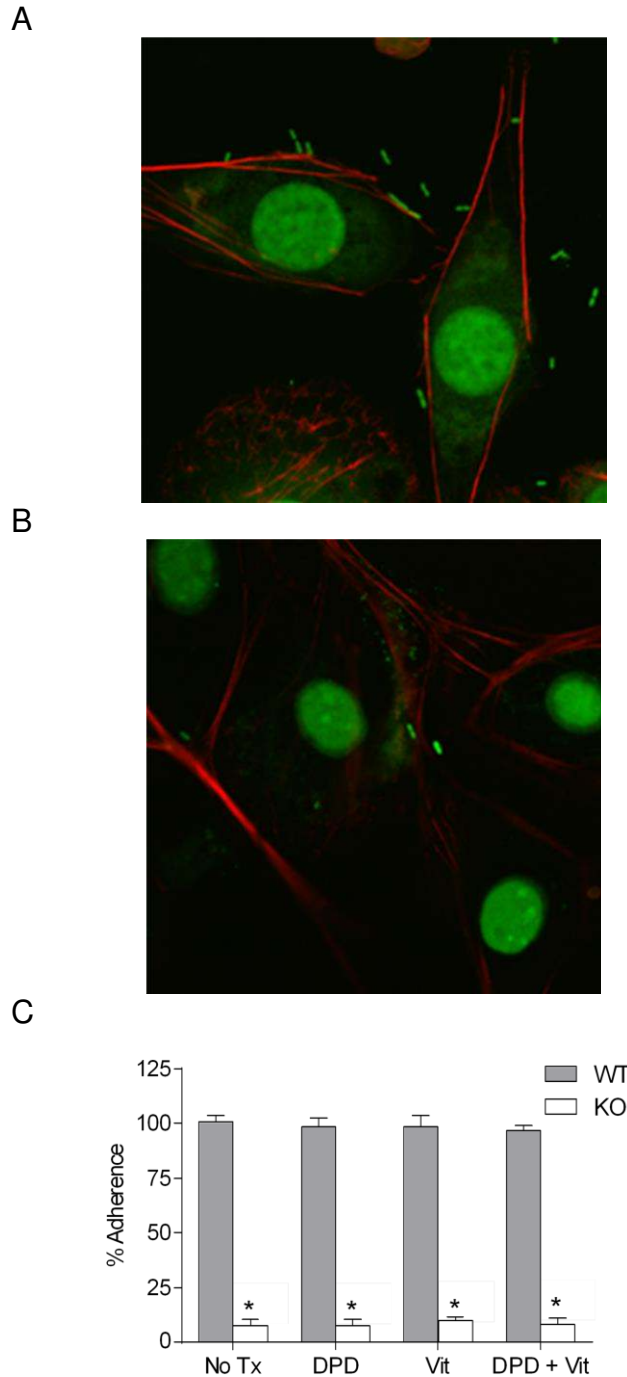


Figure 21. Analysis of *E. coli* O157:H7 WT and MTN KO strain adherence to bovine Mac-T cells. Confocal microscopy images of WT (A) and MTN KO (B) adherence to Mac-T cells. Bacteria were stained for nucleic acid (green). Mac-T cells were stained for actin (red) and nuclei (green). Bacterial adherence to Mac-T cells were determined as the CFU recovery compared to WT 3 hours post infection. MTN KO cultures were supplemented during growth with DPD, vitamin mix, or DPD and vitamin mix (* denotes $p < 0.05$ when compared to WT, \pm SEM, $n = 3$)

Shiga Toxin

One of the most deadly aspects of an *E. coli* O157:H7 infection is the high risk of developing HUS due to Shiga toxin-mediated damage to kidney endothelial cells. To better understand how MTN inhibitors may influence this type of virulence, the production of Shiga toxins in WT and MTN KO strains were compared using an African green monkey kidney epithelial (Vero) cell assay. Shiga toxin 1 (Stx1) is primarily found in the periplasmic space, whereas Shiga toxin 2 (Stx2) is secreted into the media.⁷⁰ Shiga toxin levels in cell culture supernatants and periplasmic extracts were compared for each strain. A significant decrease in cytotoxicity (~60%) was observed for culture supernatants derived from the MTN KO strain when compared to the WT strain (Figure 22 A). Culture supplementation with DPD (25 μ M) alone was insufficient to reverse the loss of cytotoxicity. When the MTN KO strain culture was supplemented with either vitamin mix (100 μ M each lipoate, thiamine, biotin) or DPD and vitamin mix (DPD + Vit), Shiga toxin mediated cytotoxicity was restored to WT levels. No significant difference was seen for Vero cell cytotoxicity in the periplasmic extracts from each strain (Figure 22 B). To ensure that differences in cytotoxicity in the assay were not masked by saturating levels of toxin, the assay was performed using a series of periplasmic extract dilutions. In general, the MTN KO strain retained more Shiga toxin activity in the periplasm than the WT strain (Figure 22 C). Culture supplementation did not result in more Shiga toxin release from the periplasm. Our results show that the MTN KO strain is still producing both Stx1 and Stx2. The increased level of periplasmic Stx in the MTN KO strain could be the result of increased expression of Stx-1 or decreased secretion of Stx-2. The effect of MTN interruption on Stx expression appears to be connected to the

nutrient status of the cells, rather than AI-2 signaling. Overall, our results suggest that MTN inhibitors could exert their antibiotic effect through decreased Shiga toxin release as one mechanism of action.

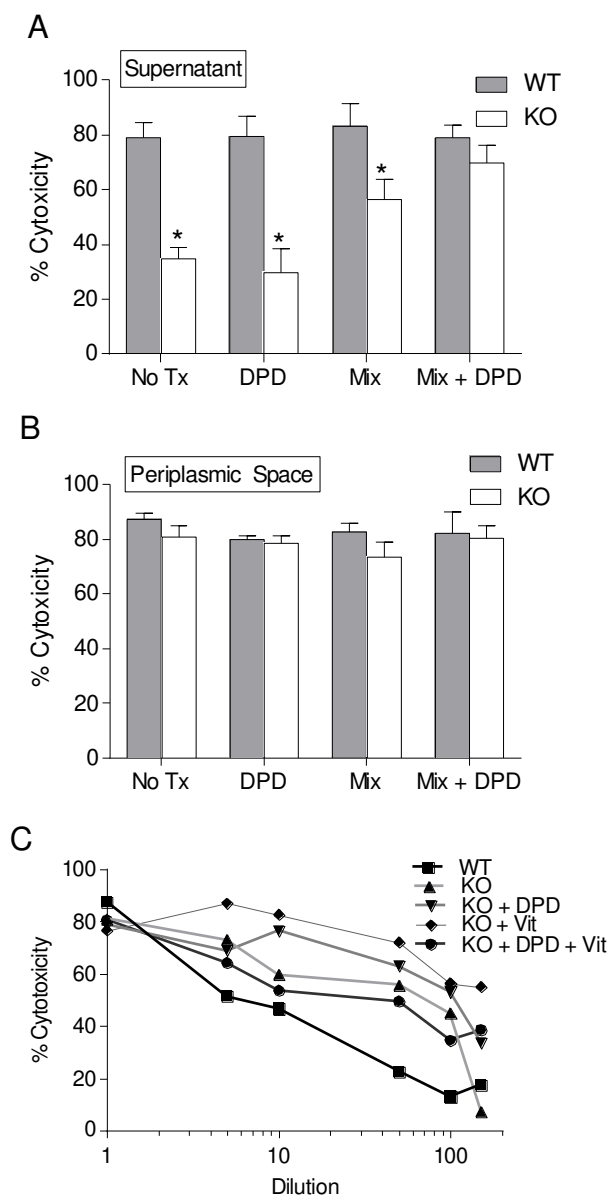


Figure 22. Effect of MTN deficiency on Shiga toxin production in *E. coli* O157:H7. Comparison of Vero cell cytotoxicity when treated with (A) culture supernatants and (B) periplasmic extracts of WT and MTN KO strains. Cultures were supplemented during growth with DPD, vitamin mix, or DPD and vitamin mix. (C) Vero cell cytotoxicity measurements using a dilution series of periplasmic extract. (* denotes $p < 0.05$ when compared to WT, \pm SEM, $n = 3$).

There have been no prior reports of Stx production in MTN KO strains. However, a *luxS* deficient strain of *E. coli* O157:H7 was reported to secrete approximately two-fold less Stx.⁸⁵ Despite this, the virulence of the strain in mice was not altered. Similarly, a *luxS* mutant of *Clostridium perfringens* produced reduced amounts of alpha-, kappa-, theta-toxins when compared to the WT strain.⁷⁸ Unfortunately, in these reports, the effect of AI-2 or nutrient supplementation was not explored so it is difficult to assess if the results were due to loss of AI-2 signaling or nutrient salvage. In any case, *luxS* deficiency would not result in the same accumulation of inhibitory nucleosides like the MTN KO strain. Thus, the effects of *luxS* deficiency do not necessarily predict the same responses that would be encountered with loss of MTN activity.

Type III Secretion System Proteins

E. coli O157:H7 produces a multitude of other virulence factors that contribute to its pathogenicity. The LEE pathogenicity island encodes many of these virulence factors, including those that are required to assemble the type III secretory system (TTSS).⁷⁶ Secretion of two specific TTSS proteins, EspB and Tir, by WT, MTN KO and MTN KI strains was analyzed by ELISA (Figure 23 A, B). EspB is a major constituent of the TTSS pore, while Tir is translocated through the pore into the host cell where it mediates subsequent bacterial adherence and pedestal formation. The MTN KO strain showed a significant decrease (20%) in EspB secretion when compared to the WT strain. EspB production was recovered to WT levels in the MTN KI strain. No significant difference was seen for the secretion of Tir. The decreased production of EspB in the MTN KO strain could result in decreased pore formation that would reduce Tir delivery to the host cell. This could be responsible for the decreased host cell adherence displayed by the

MTN KO strain (Figure 23). However, the modest decrease in EspB is likely not sufficient to account for all of the loss in adherence shown by the MTN KO strain. The TTSS contains numerous other proteins required for host cell adherence. A comprehensive investigation of the entire system is required before the effect of MTN deficiency on TTSS can be fully understood.

The TTSS has not been previously studied in MTN KO strains. The effects on TTSS proteins have been studied extensively in *luxS* mutants of *E. coli* O157:H7.^{66,76,78,79,80,83} In these studies, LEE transcription was decreased in the *luxS* mutants. Similar to our observations on the MTN KO strain, the *luxS* mutants showed a minimal ability to adhere to mammalian cells.⁷⁶ Western blot analysis of the *luxS* mutants revealed decreased expression of TTSS proteins, including EspA, EspB, and Tir responsible for the loss of mammalian cell adherence.^{66,76,78} It is unclear why there are differences in expression of Tir between the MTN KO and *luxS* mutant strains. However, the results suggest that additional factors beyond AI-2 signaling are involved in gene expression from the LEE.

Hemolysin

The final virulence factor that was investigated in this study was hemolysin. The function of hemolysin is to lyse red blood cells, which allows the bacteria to harvest the liberated iron. Hemolysin secretion by WT, MTN KO, and MTN KI strains was measured by examining the ability of cell culture supernatants to lyse sheep red blood cells. The results are expressed as a percentage of the control detergent lysis (100% control). The MTN KO strain showed a significant decrease (33%) in hemolysin activity relative to the WT and MTN KI strains (Figure 23 C). A similar finding was reported in a

luxS mutant strain of *Serratia marcescens*, where production of secreted hemolysin was reduced when compared to the WT strain. In addition, the investigators were able to fully restore hemolysin production by expression of *luxS* in trans.⁷³

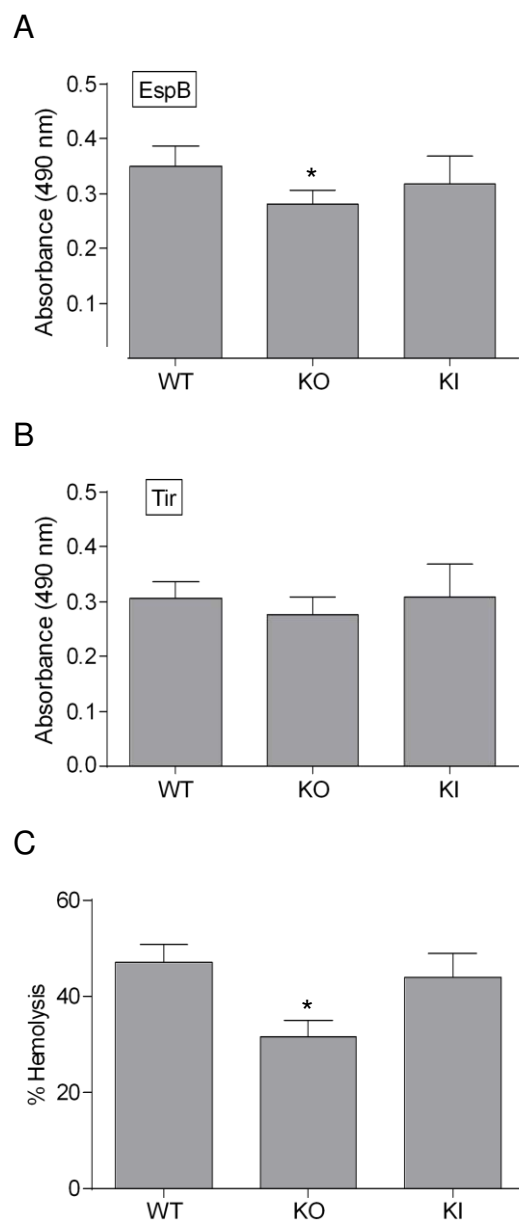


Figure 23. Comparison of virulence factor production in *E. coli* O157:H7 WT, MTN KO, and MTN KI strains. (A) ELISA analysis of secreted EspB. (B) ELISA analysis of secreted Tir. (C) Analysis of secreted hemolysin activity. (* denotes $p < 0.05$ by one-way ANOVA, \pm SEM, $n = 3$).

Overall, the MTN KO strain showed a significant decrease in virulence when compared to the parental WT strain. This provides support to the hypothesis that MTN inhibitors could act as to regulate virulence rather than directly kill bacterial cells. In reducing the ability of the pathogen to produce virulence factors, MTN inhibitors could improve the ability of the host immune system to clear infections.

Metabolic and Proteomic Analysis of *E. coli* RK4353

Prior work in our lab used nuclear magnetic resonance to examine the profiles of excreted metabolites in cell culture supernatants of the nonpathogenic *E. coli* RK4353 WT, MTN KO, and MTN KI strains. Metabolite differences were observed at mid-log and stationary phases of growth. The most notable differences were the accumulation of pyruvate (4.8 mM), lactate (0.5 mM) and glutamate (3.6 mM) in the culture supernatants of the MTN KO strain, while these compounds are scarcely detectible (<0.1 mM) in the WT and MTN KI strains. In addition, the WT and MTN KI strain cultures accumulated ethanol (0.4-0.5 mM) and acetate (4-5 mM), which are both products of vitamin (thiamine, lipoate) dependent fermentation of pyruvate. The MTN KO strain did not accumulate these compounds to the same degree (<0.1 mM ethanol; 2 mM acetate). These results suggested that there are defects in vitamin dependent central carbon metabolism in the MTN KO strain. Specifically, the pyruvate dehydrogenase complex (PDHC, lipoate-, thiamine-dependent) at the end of glycolysis and the α -ketoglutarate dehydrogenase complex (α -KDHC, lipoate-, thiamine-dependent) in the tricarboxylic acid cycle both appear to be attenuated in their activity. Thus, pyruvate accumulates in the MTN KO strain culture, or is converted through the non-vitamin dependent lactate dehydrogenase (LDH) to yield lactate. Reduced metabolic flux through α -KDHC would

lead to α -ketoglutarate being converted to 2-oxoglutarate and finally to glutamate through the non-vitamin dependent glutamate dehydrogenase pathway. The results of these studies served as the basis for our hypothesis that altered metabolism in the MTN KO strain is attributable to decreased radical SAM dependent vitamin synthesis. Since central carbon metabolism ultimately controls the ability to produce energy through oxidative phosphorylation, altered metabolism would impact growth.

Cell culture supernatants of the MTN KO strain also accumulated MTA (3-6 μ M), indicating that the nucleoside was getting secreted as a mechanism to prevent intracellular accumulation of this growth inhibitory nucleoside. As expected, MTA was absent from the WT and MTN KI strain culture supernatants, since the nucleosidase would function to efficiently catabolize the compound in these strains.

Proteomic analysis of the three nonpathogenic *E. coli* strains (WT, MTN KO, and MTN KI) was conducted at Pacific Northwest National Labs using Liquid Chromatography-Tandem Mass Spectrometry (LCMS). While not directly part of the thesis work, some of the results are presented here since they provide the rationale to support our subsequent comparison of enzyme activities in the WT, MTN KO, and MTN KI strains. The results of proteomic analysis are presented in Table 4. The MTN KO strain appears to express more PDHC and LDH proteins than the WT strain. The WT strain produced more α -KDHC and glutamate dehydrogenase than the MTN KO strain. However, a direct correlation between the protein expression and the results of the NMR analysis was not supported. It is possible that the vitamin dependent enzymes were overexpressed in the MTN KO strain, but not functionally active due to decreased vitamin synthesis in this strain.

To further investigate the results of the metabolic and proteomic experiments, multiple enzyme assays were performed. The PDHC specific activity of the cell lysate supernatants from the MTN KO strain was greatly diminished when compared to the WT strain (Figure 24 A). This would explain the accumulation of pyruvate in the MTN KO cell culture supernatants. When enzyme assays containing MTN KO cell lysates were supplemented with lipoate and thiamine, the PDHC activity was fully recovered. This supports our earlier findings that radical SAM-dependent vitamin synthesis was deficient in the MTN KO strain. Theoretically, the same situation should arise in α -KDHC as in PDHC, but we were unable to detect α -KDHC activity.

Table 4. Proteomic Differences in the WT and KO strains of *E. coli* RK4353

Protein Identification and Purpose	Fold Change*		p-value	
	Mid-Log	Stationary	Mid-Log	Stationary
<u>ADH-Alcohol Dehydrogenase</u>				
mhpF [acetaldehyde-CoA dehydrogenase II]	-3.8	-2.7	0.013	0.012
adhE [acetaldehyde: alcohol dehydrogenase]	1.1	1.3	0.642	0.337
<u>PDHC-Pyruvate Dehydrogenase Complex</u>				
aceE [pyruvate dehydrogenase, decarboxylase component E1]	-1.8	-1.7	0.054	0.061
aceF [pyruvate dehydrogenase, dihydrolipoyltransacetylase component E2]	-2	-1.9	0.022	0.037
lpd [lipoamide dehydrogenase]	-1.6	-1.7	0.004	0.023
<u>LDH- Lactate Dehydrogenase</u>				
ldhA [fermentative D-lactate dehydrogenase]	-3.3	-3.4	0.05	0.291
<u>αKDHC-α-Ketoglutarate Dehydrogenase Complex</u>				
sucB [dihydrolipoyltranssuccinase\ subunit of α -ketoglutarate DH]	1.4	-1.2	0.045	0.608
<u>GDH-Glutamate Dehydrogenase</u>				
gdhA [glutamate dehydrogenase]	1.2	1.2	0.478	0.565

* Negative values denote expression is higher in the KO strain than in the WT strain. Positive values denote a lower expression in the KO strain than the WT strain.

The MTN KO strain appears to adapt to decreased PDHC and α -KDHC by directing pyruvate and α -ketoglutarate down alternate metabolic paths. Pyruvate conversion to lactate is increased since LDH activity does not require vitamins. However, the increased flux through LDH did not require additional enzyme activity (Figure 17 B). Similarly, glutamate production was increased in the MTN KO strain, but increased GDH activity was not seen (Figure 24 D).

Lastly, while ethanol excretion was increased in the WT strain, this was not the result of increased ADH expression (Figure 24 C). Probably, the increased metabolic flux through ADH was the result of increased vitamin dependent pyruvate decarboxylase in the WT strain that subsequently increased the concentration of acetaldehyde substrate for ADH. In summary, the results of our analyses of metabolic enzymes indicate that loss of radical SAM-dependent vitamin synthesis plays a major role in metabolic adaptations in the MTN KO strain.

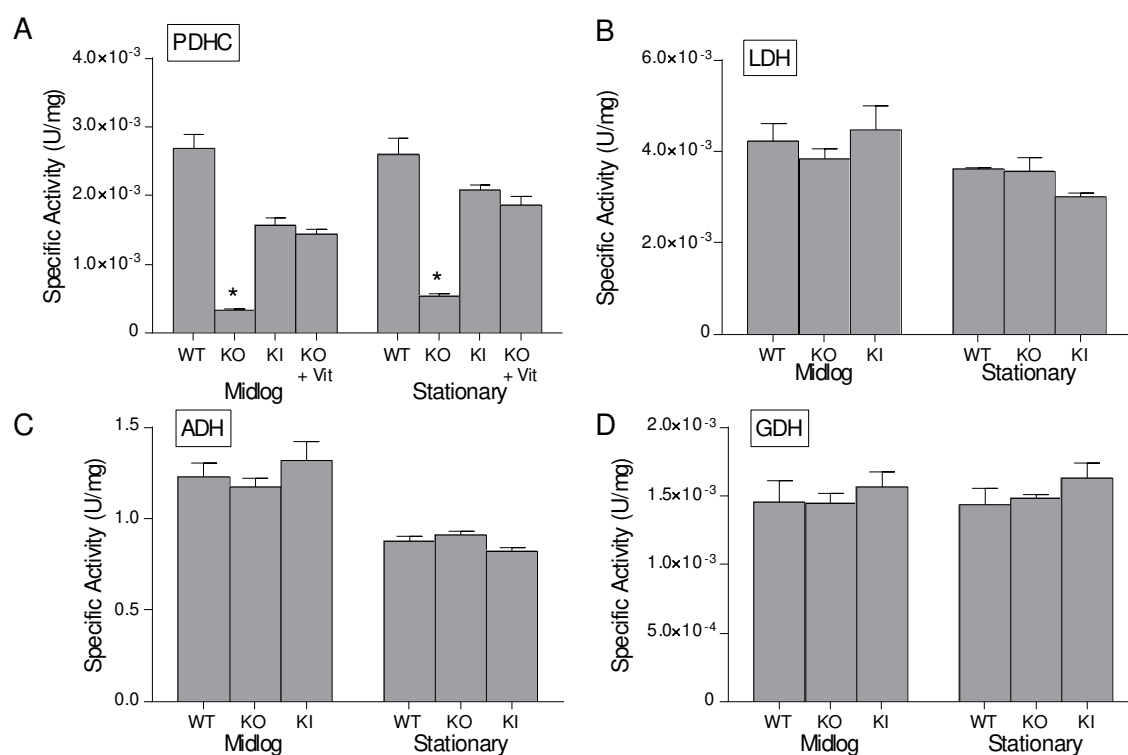


Figure 24. Analyses of the specific activities of enzymes affected by MTN deficiency in *E. coli* RK3453. (A) Pyruvate dehydrogenase complex, (B) lactate dehydrogenase, (C) alcohol dehydrogenase and (D) glutamate dehydrogenase specific activities were measured by a colorimetric assay using cell lysates from the WT, MTN KO, MTN KI strains. The specific activity of the KO strain was supplemented with lipoate and thiamine was also measured for the pyruvate dehydrogenase complex. (* denotes $p < 0.05$ when compared to WT, \pm SEM, $n = 3$)

Future Work

The work following this thesis will consist of metabolomic and proteomic analyses of the WT and MTN KO strains of *E. coli* O157:H7. Initial studies will compare this pathogenic strain to the data obtained from the nonpathogenic RK4353 strain. Analysis of various virulence factors will also be performed. Another goal is to discover other adaptations to MTN deficiency that can be identified as drug targets. The WT and KO strain of *E. coli* O157:H7 will be subjected to an array of enzyme assays to further support data found in the proteomic studies. In tandem with the LCMS analysis of virulence factors, real-time PCR investigations will be performed to understand MTN deficiency on mRNA expression. This will ultimately provide a complete understanding of MTN deficiency in a pathogenic strain of bacteria and serve as a standard comparison for MTN inhibitors.

Once the profile of MTN deficiency is established, the work will shift to testing various MTN inhibitors against the WT *E. coli* O157:H7 strain and on other bacterial species. In addition to sole inhibitor analysis, co-treatment studies with traditional antibiotics and MTN inhibitors will be performed to examine potential drug synergy. Various bacterial species that have developed resistance to most antibiotics, such as MRSA, will be treated with MTN inhibitors to determine if drug resistance can be reversed. The ultimate goal will be to test MTN inhibitors as antibiotics to treat infections in mammals (i.e., mice). This testing would provide the results needed to further pursue MTN inhibitors as antibiotic treatments in humans.

CHAPTER FOUR: CONCLUSION

Antibiotic resistance is a serious problem and eventually all forms of bacteria may become resistant to traditional antibiotics, thus making every infection potentially deadly. Due to this threat, there is a dire need for novel forms of antibiotics. A promising antibiotic target is the bacterial-specific MTN enzyme. Loss of this critical enzyme in a MTN KO strain of the pathogenic *E. coli* O157:H7 has been shown in this work to result in a significant delay in growth and reduce multiple aspects of virulence. Specifically, adherence to bovine epithelial cells was reduced by over 85% compared to the WT strain. The MTN KO strain also displayed a 60% reduction in Shiga toxin mediated cytotoxicity. Furthermore, the reduction in adherence could be partially attributed to the diminished production of TTSS proteins, in particular EspB.

Supplementation studies with DPD indicated that the alterations to growth and virulence were not due to loss of AI-2 signaling. When the MTN KO strain culture was supplemented with vitamins (lipoate, thiamine, and biotin) growth and biofilm formation was partially restored to WT levels. This suggests that the antibiotic mechanism of action for MTN inhibitors partially occurs through altered central carbon metabolism or decreases in other vitamin dependent enzyme activity. Further metabolomic and proteomic investigation of a nonpathogenic *E. coli* RK4353 strain revealed adaptations to MTN deficiency. Specific analyses of enzymes key to central carbon metabolism found an overproduction of a defective PDHC, whereas specific activity for LDH, ADH, and GDH were unchanged. The activity of the defective PDHC was restored with the addition

of lipoate and thiamine, further supporting that MTN deficiency disrupts vitamin synthesis. This study as a whole serves as the foundation for future investigations of MTN inhibitors as potential antibiotics.

REFERENCES

1. Amyes, S. G. B. *Magic Bullets Lost Horizons: The rise and fall of antibiotics*; Taylor & Francis Inc: London, 2001.
2. Fleming, A. "On the Antibacterial Action of Cultures of a *Penicillium*, with Special Reference to Their Use In the Isolation of *B. influenza*." *Brit. J. of Exp. Path.* **1929**, *10*, 226-236
3. Davies, J.; Davies, D. "Origins and evolution of antibiotic resistance." *Microbiol. Mol. Biol. Rev.* **2010**, *75*, 417-433.
4. Abraham, E. P.; Chain, E., An Enzyme from Bacteria Able to Destroy Penicillin. *Rev. Infect. Dis.* *10*:677-678. 1940.
5. Parveen, N.; Cornell, K. A. "Methylthioadenosine/S-adenosylhomocysteine Nucleosidase, a Critical Enzyme for Bacterial Metabolism." *Mol. Microbiol.* **2011**, *79*, 7-20.
6. Lu, S. C. "S-adenosylmethionine." *Int. J. Biochem. Cell Biol.* **1999**, *32*, 391-395.
7. Chiang, P. K.; Gordon, R. K.; Tal, J.; Zeng, G. C.; Doctor, B. P.; Pardhasardhi, K.; McCann, P. P. "S-Adenosylmethionine and Methylation." *FASEB J.* **1996**, *10*, 471-480.
8. Frey, P. A.; Hegeman, A. D.; Ruzicka, F. J. "The Radical SAM Superfamily." *Crit. Rev. Biochem. Mol. Biol.* **2008**, *43*, 63-88.
9. Jarrett, J. T.; "The Generation of 5'-Deoxyadenosyl Radicals by Adenosylmethionine-Dependent Radical Enzymes." *Curr. Opin. Chem. Biol.* **2003**, *7*, 174-182.
10. Challand, M. R.; Ziegert, T.; Douglas, P.; Wood, R. J.; Kriek, M.; Shaw, N. M.; Roach, P. L. "Product Inhibition in the Radical S-adenosylmethionine Family." *FEBS Lett.* **2009**, *583*, 1358-1362.
11. Igarashi, K.; Kashiwagi, K. "Modulation of Cellular Function by Polyamines." *Int. J. Biochem. Cell Biol.* **2010**, *42*, 39-51.
12. Jarrett, J. T. "The Novel Structure and Chemistry of Iron-Sulfur Clusters in the Adenosylmethionine-Dependent Radical Enzyme Biotin Synthase." *Arch. Biochem. Biophys.* **2005**, *433*, 312-321.
13. Challand, M. R.; Martins, F. T.; Roach, P. L. "Catalytic Activity of the Anaerobic Tyrosine Lyase Required for Thiamine Biosynthesis in *Escherichia coli*" **2010**, *285*, 5240-5248.
14. Cicchillo, R. M.; Booker, S. J. "Mechanistic Investigations of Lipoic Acid Biosynthesis in *Escherichia coli*: Both Sulfur Atoms in Lipoic Acid are Contributed by the Same Lipoyl Synthase Polypeptide." *J. Am. Chem. Soc.* **2005**, *127*, 2860-2861.
15. Reich, N. O.; Mashhoon, N. "Inhibition of EcoRI DNA Methylase with Cofactor Analogs." *J. Biol. Chem.* **1990**, *265*, 8066-8970.

16. Reich, N. O.; Mashhoon, N. "Kinetic Mechanism of the EcoRI DNA Methyltransferase." *Biochemistry* **1991**, *30*, 2933-2939.
17. Dorgan, K. M.; Woodechak, W. L.; Wynn, D. P.; Karschner, E. L.; Alfaro, J. F.; Cui, Y.; Zhou, Z. S.; Hevel, J. M. "An Enzyme-Coupled Continuous Spectrophotometric Assay for S-adenosylmethionine-Dependent Methyltransferases." *Anal. Biochem.* **2006**, 249-255.
18. Hendricks, C. L.; Ross, J. R.; Pichersky, E.; Noel, J. P.; Zhou, Z. S. "An Enzyme-Coupled Colorimetric Assay for S-adenosylmethionine-dependent Methyltransferases." *Anal. Biochem.* **2004**, *326*, 100-105.
19. Clarke, S.; Banfield, K. *S-adenosylmethionine-dependent methyltransferase*; Cambridge University Press: Cambridge, **2001**.
20. Pajula, R. L.; Raina, A. "Methylthioadenosine, A Potent Inhibitor of Spermine Synthase From Bovine Brain." *FEBS Lett.* **1979**, *99*, 343-345.
21. Raina, A.; Tuomi, K.; Rajula, R. L. "Inhibition of the Synthesis of Polyamines and Macromolecules by 5'-Methylthioadenosine and 5'-Alkylthiotubercidins in BHK21 Cells." *Biochem. J.* **1982**, *204*, 697-703.
22. Hanzelka, B. L.; Parsek, M. R.; Val, D. L.; Dunlap, P. V.; Cronan, J. E. Jr.; Greenberg, E. P. "Acylhomoserine Lactone Synthase Activity of the *Vibrio fischeri* AinS Protein." **1999**, *181*, 5766-5770.
23. Lee, J. E.; Cornell, K. A.; Riscoe, M. K.; Howell, P. L. "Structure of *E. coli* 5'-methylthioadenosine/S-adenosylhomocysteine Nucleosidase Reveals Similarity to the Purine Nucleoside Phosphorylase." *Structure* **2001**, *10*, 941-953.
24. Sun, J.; Daniel, R.; Wagner-Döbler, I.; Zeng, A. P. "Is Autoinducer-2 a Universal Signal for Interspecies Communication: A Comparative Genomic and Phylogenetic Analysis of the Synthesis and Signal Transduction Pathways." *BMC Evol. Biol.* **2004**, *4*, 36.
25. Sekowska, A.; Dénervaud, V.; Ashida, H.; Michoud, K.; Haas, D.; Yokota, A.; Danchin, A. "Bacterial Variations on the Methionine Salvage Pathway." *BMC Microbiol.* **2004**, *4*, 9.
26. Cornell, K. A.; Swarts, W. E.; Barry, R. D.; Riscoe, M. K.; "Characterization of Recombinant *Escherichia coli* 5'-Methylthioadenosine/S-adenosylhomocysteine Nucleosidase: Analysis of Enzymatic Activity and Substrate Specificity." *Biochem. Biophys. Res. Commun.* **1996**, *228*, 724-732.
27. Cacciapuoti, G.; Bertoldo, C.; Brio, A.; Zappia, V.; Porcelli, M. "Purification and Characterization of 5'-methylthioadenosine Phosphorylase from the Hyperthermophilic Archaeon *Pyrococcus furiosus*: Substrate Specificity and Primary Structure Analysis." *Extremophiles* **2003**, *7*, 159-168.
28. Stepkowski, T.; Brzeziński, K.; Legocki, A. B.; Jaskólski, M.; Béna, G. "Bayesian Phylogenetic Analysis Reveals Two-domain Topology of S-adenosylhomocysteine Hydrolase Protein Sequences." *Mol. Phylogenet. Evol.* **2005**, *34*, 15-28.
29. Cornell, K. A.; Riscoe, M. K.; "Cloning and Expression of *Escherichia coli* 5'-methylthioadenosine/S-adenosylhomocysteine nucleosidase: Identification of the *pfs* gene." *Biochim. Biophys. Acta.* **1998**, *1396*, 8-14.

30. Furfine, E. S.; Abeles, R. H. "Intermediates in the Conversion of 5'-S-Methylthioadenosine to Methionine in *Klebsiella pneumoniae*." *J. Biol. Chem.* **1988**, *263*, 9598-95606.
31. Singh, V.; Evans, G. B.; Lenz, D. H.; Mason, J. M.; Clinch, K.; Mee, S.; Painter, G. F.; Tyler, P. C.; Furneaux, R. H.; Lee, J. E.; Howell, P. L.; Schramm, V. L. "Femtomolar Transition State Analogue Inhibitors of 5'-Methylthioadenosine/S-Adenosylhomocysteine Nucleosidase from *Escherichia coli*." *J. Biol. Chem.* **2005**, *18*, 18265-18273.
32. Hughes, J. A. "In vivo Hydrolysis of S-adenosyl-L-methionine in *Escherichia coli* Increases Export of 5-methylthioribose." *Can. J. Microbiol.* **2006**, *52*, 599-602.
33. Kamarthapu, V.; Rao, K. V.; Srinivas, P. N.; Reddy, G. B.; Reddy, V. D. "Structural and Kinetic Properties of *Bacillus subtilis* S-adenosylmethionine Synthetase Expressed in *Escherichia coli*." **2008**, *1784*, 1949-1958.
34. Ferro, A. J.; Barrett, A.; Shapiro, S. K. "Kinetic Properties and the Effect of Substrate Analogues on 5'-methylthioadenosine Nucleosidase from *Escherichia coli*." *Biochim. Biophys. Acta.* **1976**, *438*, 487-494.
35. Lee, J. E.; Cornell, K. A.; Riscoe, M. K.; Howell, P. L. "Structure of *Escherichia coli* 5'-Methylthioadenosine/S-Adenosylhomocysteine Nucleosidase Inhibitor Complexes Provide Insight into the Conformational Changes Required for Substrate Binding and Catalysis." *J. Biol. Chem.* **2003**, *278*, 8761-8770.
36. Lee, J. E.; Settembre, E. C.; Cornell, K. A.; Riscoe, M. K.; Sufrin, J. R.; Ealick, S. E.; Howell, P. L. "Structural Comparison of MTA Phosphorylase and MTA/AdoHcy Nucleosidase Explains Substrate Preferences and Identifies Regions for Exploitable for Inhibitor Design." *Biochemistry* **2004**, *43*, 5159-5169.
37. Lee, J. E.; Smith, G. D.; Horvatin, C.; Huang, D. J.; Cornell, K. A.; Riscoe, M. K.; Howell, P. L. "Structural Snapshots of MTA/AdoHcy Nucleosidase Along the Reaction Coordinate Provide Insights into Enzyme and Nucleosidase Flexibility During Catalysis." *J. Mol. Biol.* **2005**, *352*, 559-574.
38. Singh, V.; Lee, J. E.; Núñez, S.; Howell, P.; Schramm, V. L. "Transition State Structure of 5'-Methylthioadenosine/S-adenosylhomocysteine Nucleosidase from *Escherichia coli* and Its Similarity to Transition State Analogues." *Biochemistry* **2005**, *44*, 11647-11659.
39. Longshaw, A. I.; Adanitsch, F.; Gutierrez, J. A.; Evans, G. B.; Tyler, P. C.; Schramm, V. L. "Design and Synthesis of Potent "Sulfur-Free" Transition State Analogue Inhibitors of 5'-Methylthioadenosine Nucleosidase and 5'-Methylthioadenosine Phosphorylase." *J. Med. Chem.* **2010**, *53*, 6730-6746.
40. Schramm, V. L.; Gutierrez, J. A.; Cordovano, G.; Basu, I.; Guha, C.; Belbin, T. J.; Evans, G. B.; Tyler, P. C.; Furneaux, R. H. "Transition State Analogues in Quorum Sensing and SAM recycling." *Nucleic. Acids Symp. Ser. (Oxf.)* **2008**, *52*, 75-76.
41. Cornell, K. A.; Primus, S.; Martinez, J. A.; Parveen, N. "Assessment of Methylthioadenosine/S-adenosylhomocysteine nucleosidases of *Borrelia burgdorferi* as Targets for Novel Antimicrobials Using a Novel High-throughput Method." *J. Antimicrob. Chemother.* **2009**, *63*, 1163-1172.
42. Halliday, N. M.; Hardie, K. R.; Willaims, P.; Winzer, K.; Barrett, D. A. "Quantitative Liquid Chromatography–Tandem Mass Spectrometry Profiling of

- Activated Methyl Cycle Metabolites Involved in LuxS-dependent Quorum Sensing in *Escherichia coli*." **2010**, *403*, 20-29.
43. Heurlier, K.; Vendeville, A.; Halliday, N.; Green, A.; Winzer, K.; Tang, C. M.; Hardie, K. R. "Growth Deficiencies of *Neisseria meningitidis* *pfs* and *luxS* Mutants Are Not Due to Inactivation of Quorum Sensing." *J. Bacteriol.* **2009**, *191*, 1293-1302.
 44. Winzer, K.; Sun, Y. H.; Green, A.; Delory, M.; Blackley, D.; Hardie, K. R.; Baldwin, T. J.; Tang, C. M. "Role of *Neisseria meningitidis* *luxS* in Cell-to-Cell Signaling and Bacteremic Infection." *Infect. Immun.* **2002**, *70*, 2245- 2248.
 45. Rutherford, S. T.; Bassler, B. L. W. A. "Bacterial Quorum Sensing: Its Role in Virulence and Possibilities for Its Control." *Cold Spring Harbor Perspect Med* **2012**, *2*, 1-25.
 46. Miller, M. B.; Bassler, B. L. "Quorum Sensing in Bacteria." *Annu. Rev. Microbiol.* **2001**, *55*, 165-199.
 47. Pereira, C. S.; Thompson, J. A.; Xavier, K. B. "AI-2-Mediated Signaling in Bacteria." *FEMS Microbiol. Rev.* **2013**, *37*, 156-181.
 48. Sun, J.; Daneil, R.; Wagner-Döbler, I.; Zeng, A. P. "Is Autoinducer-2 a Universal Signal for Interspecies Communication." *BMC Evol. Biol.* **2004**, *4*, 36.
 49. Marques, J. C.; Lamosa, P.; Russell, C.; Ventura, R.; Maycock, C.; Semmelhack, M. F.; Miller, S. T.; Xavier, K. B. "Processing the Interspecies Quorum-Sensing Signal Autoinducer-2 (AI-2): Characterization of Phospho-(S)-4,5-dihydroxy-2,3-pentanedione isomerization by LsrG protein." *J. Biol. Chem.* **2011**, *286*, 18331-18343.
 50. Chen, X.; Schauder, S.; Potier, N.; Van Dorsselaer, A.; Pelczer, I.; Bassler, B. L.; Hughson, F. M. "Structural Identification of a Bacterial Quorum-Sensing Signal Containing Boron." *Nature* **2002**, *415*, 545-549.
 51. Antunes, L. C.; Ferreira, R. B.; Buckner, M. M.; Finlay, B. B. "Quorum Sensing in Bacterial Virulence." *Microbiology* **2010**, *156*, 2271-2282.
 52. Hardie, K. R.; Heurlier, K. "Establishing Bacterial Communities by 'Word of Mouth': LuxS and Autoinducer 2 in Biofilm Development." *Nat. Rev. Microbiol.* **2008**, *6*, 635-643.
 53. Watnick, P.; Kolter, P. "Biofilm, City of Microbes." *J. Bacteriol.* **2000**, *182*, 2675-2679.
 54. Costerton, J. W.; Stewart, P. S.; Greenberg, E. P. "Bacterial Biofilms: A Common Cause of Persistent Infections." *Science*, **1999**, *284*, 1318-1322.
 55. Jesaitis, A. J.; Franklin, M. J.; Berglund, D.; Sasaki, M.; Lord, C. I.; Bleazard, J. B.; Duffy, J. E.; Beyenal, H.; Lewandowski, Z. "Comprised Host Defense on *Pseudomonas aeruginosa* Biofilms: Characteristic of Neutrophil and Biofilm Interactions." *J. Immunol.* **2003**, *171*, 4329-4339.
 56. Ferens, W. A.; Hovde, C. J. "*Escherichia coli* O157:H7: Animal Reservoir and Sources of Human Infection." *Foodborne Pathogens and Disease* **2011**, *4*, 465-487.
 57. Law, D. "Virulence Factors of *Escherichia coli* O157 and Other Shiga Toxin-producing *E. coli*." *J. Appl. Microbio.* **2000**, *88*, 729-745.
 58. Riley, L. W.; Remis, R. S.; Helgerson, S. D.; McGee, H. B.; Wells, J. G.; Davis, B. R.; Hebert, R. J.; Olcott, E. S.; Johnson, L. M.; Hargrett, N. T.; Blake, P. A.;

- Cohen, M. L. "Hemorrhagic Colitis Associated with a Rare *Escherichia coli* Serotype" *N. Engl. J. Med.* **1983**, *308*, 681-685.
59. Michino, H.; Araki, K.; Minami, S.; Nakayama, T.; Ejima, Y.; Hiroe, K. "Recent Outbreaks of Infections Caused by *Escherichia coli* O157:H7 in Japan." *Amer. Soc. Microbiol.* **1998**, 73-81.
 60. Karch, H.; Tarr, P. I.; Bielaszewska, M. "Enterohaemorrhagic *Escherichia coli* in Human Medicine." *Int. J. Med. Microbiol.* **2005**, *295*, 405-418.
 61. O'Brien, A. D.; Holmes, R. K. "Shiga and Shiga-Like Toxins." *Microbiol. Rev.* **1987**, *51*, 206-220.
 62. Sandvig, K.; van Deurs, D. "Endocytosis Intracellular Transport and Cytotoxic Action of Shiga Toxin and Ricin." *Physiol. Rev.* **1996**, *76*, 949-966.
 63. He, S. Y.; Nomura, K.; Whittman, T. S. "Type III Protein Secretion Mechanism in Mammalian and Plant Pathogens." *Biochem. Biophys. Acta.* **2004**, *1694*, 181-206.
 64. Li, Y.; Frey, E.; Mackenzie, A. M.; Finlay, B. B. "Human response to *Escherichia coli* O157:H7 infection: Antibodies to Secreted Virulence Factors." *Infect. Immun.* **2000**, *68*, 5090-5095.
 65. Kenny, B.; DeVinney, R.; Stein, M.; Reinscheid, D. J.; Frey, E. A.; Finaly, B. B. "Enteropathogenic *E. coli*(EPEC) Transfers Its Receptor for Intimate Adherence into Mammalian Cells." *Cell* **1997**, *91*, 511-520.
 66. Lim, J. Y.; Yoon, J.; Hovde, C. J. "A Brief Overview of *Escherichia coli* O157:H7 and Its Plasmid O157." *J. Microbiol. Biotechnol.* **2010**, *20*, 5-14.
 67. Sperandio, V.; Torres A. G., Jarvis, B.; Nataro, J. P.; Kaper, J. B. "Bacteria-Host Communication: The Language of Hormones." *Proc. Natl. Acad. Sci. USA* **2003**, *100*, 8951-8956.
 68. Cadieux, N.; Bradbeer, C. Reeger-Schneider, E.; Köster, W.; Mohanty, A. K.; Wiener, M. C.; Kadner, R. J. "Identification of the Periplasmic Cobalamin-Binding Protein BtuF of *Escherichia coli*." *J. Bacteriol.* **2002**, *184*, 706-717.
 69. Arval, U. K.; Stöckel, J.; Krowidi, R. K.; Gritsenko, M. A.; Monroe, M. E.; Moore, R. J.; Koppelaar D. W.; Smith, R. D.; Pakrasi, H. B.; Jacobs, J. M. "Dynamic Proteomic Profiling of a Unicellular Cyanobacterium *Cyanothece* ATCC51142 across Light-Dark Diurnal Cycles." *BMC Syst. Biol.* **2011**, *5*, 194.
 70. Shimizu, T.; Ohta, Y.; Noda, M.; "Shiga-toxin 2 Is Specifically Released from Bacterial Cells by Two Different Mechanisms." *Infect. Immun.* **2009**, *7*, 2813-2823.
 71. Gutierrez, J. A.; Crowder, T.; Rinaldo-Matthis, A.; Ho, M.; Almo, S. C.; Schramm. "Transition State Analogues of 5'-Methylthioadenosine Nucleosidase Disrupt Quorum Sensing." *Nat. Chem. Biol.* **2009**, *4*, 251-257.
 72. Barrios, A. F. G.; Zuo, R.; Hashimoto, Y.; Yang, L.; Bentley, W. E.; Wood, T. K. "Autoinducer 2 Controls Biofilm Formation in *Escherichia coli* through a Novel Motility Quorum-Sensing Regulator." *J. Bacteriol.* **2006**, *188*, 305-316.
 73. Coulthurst, S. J.; Kurz, C. L.; Slamond, G. P. "*luxS* Mutants of *Serratia* Defective in Autoinducer-2-dependent 'Quorum Sensing' Show Strain-dependent Impacts on Virulence and Production of Carbapenem and Prodigiosin." *Microbiology* **2004**, *150*, 1901-1920.

74. Merritt, J.; Qi, F.; Goodman, S. D.; Anderson M. H.; Shi, W. "Mutation of *luxS* Affects Biofilm Formation in *Streptococcus mutans*." *Infect. Immun.* **2003**, *71*, 1972-1979.
75. Lyon, W. R.; Madden, J. C.; Levin, J. C.; Stein, J. L.; Caparon, M. G. "Mutation of *luxS* Affects Growth and Virulence Factor Expression in *Streptococcus pyogenes*." *Mol. Microbiol.* **2001**, *42*, 145-157.
76. Vendeville, A.; Winzer, K.; Heurlier, K.; Tang, C. M.; Hardie, K. R. "Making 'Sense' of Metabolism: Autoinducer-2, *luxS* and Pathogenic Bacteria." *Nat. Rev. Microbiol.* **2005**, *3*, 383-396.
77. Sircili, M. P.; Walters, M.; Trabulsi, L. R.; Sperandio, V. "Modulation of Enteropathogenic *Escherichia coli* Virulence by Quorum Sensing" *Infect. Immun.* **2004**, *72*, 2329-2337.
78. Ohtani, K.; Hayashi, H.; Shimizu, T. "The *luxS* Gene is Involved in Cell-Cell Signalling for Toxin Production in *Clostridium perfringens*." *Mol. Microbiol.* **2002**, *44*, 171-179.
79. Sperandio, V.; Li, C. C.; Kaper, J. B. "Quorum-Sensing *Escherichia coli* Regulator A: a Regulator of the LysR Family Involved in the Regulation of the Locus of Enterocyte Effacement Pathogenicity Island in Enterohemorrhagic *E. coli*." *Infect. Immun.* **2002**, *70*, 3085-3093.
80. Sperandio, V.; Mellies, J. L.; Nguyen, W.; Shin, S.; Kaper, J. B. "Quorum Sensing Controls Expression of the Type III Secretion Gene Transcription and Protein Secretion in Enterohemorrhagic and Enteropathogenic *Escherichia coli*." *Proc. Natl. Acad. Sci. USA* **1999**, *96*, 15196-15201.
81. Tavender, T. J.; Halliday, N. M.; Hardie, K. R.; Wizner, K. "LuxS-independent Formation of AI-2 from Ribulose-5-phosphate." *BMC Microbiol.* **2008**, *8*, 98
82. Choi-Rhee, E.; Cronan, J. E. "A Nucleosidase Required for *in vivo* Function of the S-adenosyl-L-methionine Radical Enzyme, Biotin Synthase." *Chem. Biol.* **2005**, *12*, 589-593.
83. Perrett, C. A.; Karvolos, M. H.; Humphrey, S.; Mastroeni, P.; Martinez-Argudo, I.; Spencer, H.; Bulmer, D.; Winzer, K.; McGhie, E.; Koronakis, V.; Williams, P.; Khan, C. M.; Jepson, M. A. "LuxS-based Quorum Sensing Does Not Affect the Ability of *Salmonella enterica* serovar *Typhimurium* to Express the SPI-1 Type 3 Secretion, Induce Membrane Ruffles, or Invade Epithelial Cells." *J. Bacteriol.* **2009**, *191*, 7253-7259.
84. Monroe, D. "Looking for Chinks in the Armor of Bacterial Biofilms." *PLoS Biol.* **2007**, *5*, 307.
85. Jeon, B.; Itoh, K. "Production of Shiga Toxin By a *luxS* Mutant of *Escherichia coli* O157:H7 *in vivo* and *in vitro*." *Microbiol. Immunol.* **2007**, *51*, 391-396.
86. Sperandio, V.; Torres, A. G.; Giron, J. A.; Kaper, J. B. "Quorum Sensing is a Global Regulatory Mechanism in Enterohemorrhagic *Escherichia coli* O157:H7." *J. Bacteriol.* **2001**, *183*, 5187-5197.
87. George, E. A.; Muir, T. W. "Molecular Mechanisms of *agr* Quorum Sensing in Virulent Staphylococci." *Chem. Bio. Chem.* **2007**, *8*, 847-855.
88. Singh, A.; Del Poeta, M. "Lipid Signalling in Pathogenic Fungi." *Cell Microbiol.* **2011**, *13*, 177-185

89. Duerre, J. A.; Ribi, E. "Enzymes Released from *Escherichia coli* with the Aid of A Servall Cell Fractionator." *Appl. Microbiol.* **1963**, *11*, 467-471.
90. Datsenko, K. A.; Wanner, B. L. "One-step Inactivation of Chromosomal Genes in *Escherichia coli* K-12 using PCR Products." *Proc. Natl. Acad. Sci. USA* **2000**, *97*, 6640-6645.
91. Sampathkumar, B.; Tsougriani, E.; Yu, L. S. L.; Khachatourians, G. C. "A Quantitative Microtiter Plate Hemolysis Assay for *Listeria monocytogenes*." *J. Food Saft.* **1998**, *18*, 197-203.
92. Xavier, K. B.; Bassler, B. L.; "LuxS Quorum Sensing: More Than Just a Numbers Game." *Curr. Opin. Microbiol.* **2003**, *6*, 191-197.
93. Merrit, J. H.; Kadouri, D. E.; O'Toole, G. A.; "Growing and Analyzing Static Biofilms." *Curr. Protoc. Microbiol.* **2005**, *22*, 1B.1.1-1B.1.18.
94. Puttamreddy, S.; Minion, F. "Linkage Between Cellular Adherence and Biofilm Formation in *Escherichia coli* O157:H7 EDL933." *Fed. Eur. Microbiol. Soc.* **2010**, *315*, 46-53.
95. Dixon, R. A.; Chopra, I. "Leakage of Periplasmic Proteins from *Escherichia coli* Mediated by Polymyxin B Nonapeptide." *Antimicrob. Agents. Chemother.* **1986**, *29*, 781-788.
96. Babson, A. L.; Basbon, S. R. "Kinetic Color Measurement of Serum Lactate Dehydrogenase Activity." *Clin. Chem.* **1973**, *19*, 766-769.
97. Defoirdt, T.; Boon, N.; Bossier, P. "Can Bacteria Evolve Resistance to Quorum Sensing Disruption." *PLoS Pathog.* **2010**, *6*, 1-6.